Precision QCD propagators with dynamical quarks from the Curci-Ferrari model

Nahuel Barrios,[1,2] John A. Gracey,[3] Marcela Peláez,[1] and Urko Reinosa[2]

[1] *Instituto de Física, Facultad de Ingeniería, Universidad de la República,*
J. H. y Reissig 565, 11000 Montevideo, Uruguay.

[2] *Centre de Physique Théorique (CPHT), CNRS, Ecole Polytechnique,*
Institut Polytechnique de Paris, Route de Saclay, F-91128 Palaiseau, France.

[3] *Theoretical Physics Division, Department of Mathematical Sciences,*
University of Liverpool, P.O. Box 147, Liverpool, L69 3BX, United Kingdom

(Dated: March 31, 2021)

We evaluate all two-point correlation functions of the Curci-Ferrari (CF) model in four dimensions and in the presence of degenerate fundamental quark flavors. We compare our results to QCD lattice data in the two flavor case for two different values of the pion mass, one that is relatively far from the chiral limit, and one that is closer to the physical value. This work is a natural extension of an earlier investigation in the quenched approximation. Our results confirm that the QCD gluon and ghost dressing functions are well described by a perturbative approach within the CF model. As for the quark sector, our main result is that the quark dressing function is also well captured by the perturbative approach, but only starting at two-loop order, as anticipated in Ref. [1]. The quark mass function is also well reproduced if the quarks are not too light. As is well known, this function cannot be described within a purely perturbative approach in the case of too light quarks. We find nonetheless that, provided one allows for a small offset in the UV, the quark mass function is rather well reproduced in the IR, even for physical quark masses. We also find that, for a given quark mass in the UV, the two-loop corrections tend to generate more mass in the infrared than the one-loop corrections.

I. INTRODUCTION

The success of the Standard Model of particle physics in describing three out of the four fundamental interactions is not in any doubt. Nonetheless, while the properties of the electroweak sector are very well understood over a large range of energies, that part describing the strong sector is not. At high energy, the quarks and gluons that are the fundamental fields of the $SU(3)$ gauge theory of the strong sector, known as Quantum Chromodynamics (QCD), behave asymptotically as free entities, [2, 3]. This is only a high energy property, however, as in reality such quark and gluon states are never realized in Nature as observable particles. Instead they are confined within nucleons and from lattice gauge studies of their propagators, it has become clear that they do not share the same fundamental behaviour as the electrons and photons of Quantum Electrodynamics. A distinctive feature is that, as a function of the momentum p^2 the propagators do not have a simple real pole. See, for instance, [4–12].

Consequently there have been numerous theoretical attempts to explain the behaviour of the gluon propagator analytically. The most common approaches rely on non-perturbative methods such as the Dyson-Schwinger equations [13] or the functional renormalization group [14]. Alongside these non-perturbative studies, it has also been advocated that valuable information could be obtained from perturbative methods [15]. All these approaches centre around a common theme of there being a non-zero mass scale of some sort that is active primarily at low energies.

Ideally, one aims at generating this scale from first principles, as for instance in the original work of Gribov, [16], where it arose out of endeavouring to globally fix the Landau gauge uniquely. A more phenomenological approach relies on the inclusion of a non-zero gluon mass term in the Landau gauge-fixed Lagrangian as a way to model the effect of the non-perturbative gauge-fixing. This model corresponds in fact to one particular case of the so-called Curci-Ferrari (CF) model [17]. That approach from nearly half a century ago fell out of favour despite the modified Yang-Mills (YM) Lagrangian being renormalizable. It transpired that the BRST charge is not nilpotent in the presence of the explicit mass. Consequently the standard definition of the physical state space contained states with negative norm [18–20]. Since then, however, it has been shown in lattice simulations that the gluon propagator features positivity violation [21, 22]. This empirical observation together with the decoupling behaviour of the gluon propagator observed for dimensions strictly greater than 2 [23, 24] has made the CF model one new avenue for exploring the infrared behaviour of the gluon and Faddeev-Popov ghost propagators. This is one of the main motivations for continuing to study the model in this article.

Indeed over the past years the CF model has been extensively used to examine the infrared behaviour of YM/QCD correlation functions in the vacuum [1, 15, 25, 26] as well as the phase structure at nonzero temperature [27–33], both from a perturbative perspective. One of the reasons why the model may be regarded as a credible

candidate for describing infrared gluon dynamics is that in [34, 35] it was argued that the mass parameter can be interpreted as a necessary second gauge parameter. Its origin derives from taking into account the presence and effect of Gribov copies; see also [36] for more recent developments. In the ultraviolet, such a mass is unnecessary and absent as it runs to zero consistent with the fact that the Landau gauge is uniquely fixed in that region. While the one loop studies of the gluon and ghost propagators using the CF model [1, 26] were very encouraging and gave good coverage of lattice data to all energies, the natural question that arose concerned whether this could be improved if higher loop corrections were included. This was examined at two loops in Ref. [37] for the case of YM two-point correlation functions where a much closer agreement with lattice data over all momenta emerged. While this does not imply that a gluon mass term should be included in Landau gauge-fixed YM theory, it did at least demonstrate that perturbative computations could be used to quantitatively probe the deeper infrared regions of pure YM theory that at first might not seem possible. More recently, a similar investigation was pursued for the case of the ghost-antighost-gluon vertex in one particular momentum configuration [39], with the added difficulty that all relevant parameters had been fixed in Ref. [37], thus representing a stringent test of the method.

Having demonstrated that a gluon mass term gives a window into the infrared the next natural extension of this core idea is to include massive quarks on top of the YM gluon mass term of the CF model and thereby endeavour to access QCD in the infrared. Of course, including a quark mass one aims at probing chiral symmetry breaking, another aspect of the infrared that is not fully understood. This is certainly a challenge in particular within the CF model as one needs to consider the quark wave (or dressing) function and the quark mass function as extra form factors on top of the gluon and ghost dressing functions. Moreover, all these form factors depend a priori on two mass scales.

A one-loop investigation of the CF model in the presence of massive quarks was carried out in Ref. [1]. Given the extension of Ref. [37] the main direction of this article is to extend the work of Ref. [1] to two loops. There are at least two other reasons for considering the two-loop extension. First, in Ref. [1], it was not easy to obtain full satisfactory results at one loop in the Landau gauge. Indeed, in this gauge, the quark field does not need to be renormalized at one loop. This is because the one loop correction to the wave function part of the quark two-point function is finite. In fact for massless fields it vanishes identically in the Landau gauge. In effect this meant that the quark wave form factor could not be commensurate with the other form factors which was evident in Ref. [1] from the clear qualitative mismatch between the CF one-loop predictions for this quantity and the corresponding lattice results. Therefore to extract results that are meaningful at the same level of precision

as [37] for instance, a full *two* loop study is absolutely necessary. In fact an estimate of the two-loop corrections to this quantity given in Ref. [1] indicates that they could greatly contribute to resolve the tension with the lattice data. One of the goals of the present paper is to show that this is indeed what happens and therefore that just as the gluon and ghost correlators, the quark wave function admits an accurate description within the perturbative CF paradigm.

The second reason for considering the two-loop extension is that, despite the evidence for an accurate description of YM correlation functions within the perturbative CF model, the situation in QCD is more delicate. Indeed, given that the quark gluon coupling in the infrared is two to three times larger than the pure gauge coupling [38], the use of a strict perturbative approach is certainly questionable and one way to test it is to evaluate the size of the two-loop corrections. In fact, as it is well known, the quark mass function cannot be reproduced perturbatively in the chiral limit. Still, it makes sense to ask whether other QCD form factors are well described within the perturbative CF approach. One of the ideas to be defended in this work is that both the gluon and the ghost form factors, but also the quark wave form factor can be accurately captured perturbatively, and this when even close to the chiral limit.

For completeness, we mention that it is also possible to account for the spontaneous breaking of chiral symmetry and the quark mass form factor within the CF model. To do so, one needs to abandon the perturbative expansion scheme and replace it by a double expansion in powers of the pure gauge coupling (that remains moderate over all scales in the CF model) and the inverse number of colors. This has led to the development of the so-called Rainbow-Improved expansion scheme [41, 42] that essentially boils down, at leading order, to the Rainbow-Ladder approximation (see e.g. [43, 44]) while consistently including the running of the parameters. In has been shown that this approximation scheme captures the spontaneous chiral symmetry breaking and provides a consistent picture of the gluon and ghost propagators as well as the quark mass function.[1] This goes, however, beyond the scope of the present work and we will remain at a strict two-loop order.

While one could argue that perturbation theory should not be used for such studies, one point of view is that one is trying to probe beyond the leading order high energy behaviour where in effect quarks and certainly gluons are massless. More usefully it in principle gives a technique to carry out more phenomenological studies for medium

----

[1] The quark wave function is poorly reproduced at leading order of the Rainbow-Improved expansion basically for the same reason as the one described in the main text: just as in the one-loop case, there is no wave function renormalization of the propagator and then the quark wave function cannot be commensurate with the other form factors.

to low energies similar to those begun in [45, 46] for instance where a dynamical gluon mass was used. While there are Dyson-Schwinger analyses of the quark wave function and mass form factors in Ref. [47, 48] for example, see also [49] for more recent and thorough results, perturbative approaches such as that provided here should be regarded as complementary. This is in the sense that in any theoretical exploration of the infrared, some degree of modelling and approximations has to be made. In ours it is clearly the loop expansion (on top of the CF modelling) which in principle can be extended to three loops with the development of numerical tools to evaluate the underlying Feynman integrals for example.

Going to two-loop order in the present set-up is not a straightforward task. In Ref. [37] the focus was on pure YM where there was only one mass scale. Here we will have two distinct masses when the dynamical quarks are included. Therefore we have to evaluate all possible two loop massive Feynman integrals contributing to the gluon, ghost and quark two-point functions in the Landau gauge. Indeed aside from the one loop correction to the quark two-point function, it is not until two loops that graphs with both mass scales are present in individual diagrams. It is only at this point that we truly have a tool to fully explore the interrelationship between the mass parameters behind color confinement and chiral symmetry breaking.

The paper is organized as follows. We provide the necessary background details for the Curci-Ferrari model we use in Section II. This includes the definition of the form factors that are computed to two loops as well as a general review of the finer points of the renormalization scheme that allows us to probe the infrared. A summary of the one loop work of Ref. [1] is also provided together with the definition of the Infrared Safe renormalization scheme to be used throughout this work. The following section describes the technical aspects of calculating the necessary two loop Feynman graphs contributing to each of the two-point functions when there are two independent mass scales. As our ultimate goal is to plot the form factors for all momenta a substantial part of the discussion is devoted to internal checks in various limits that ensure the results are reliable prior to constructing plots. The implementation of the Infrared Safe renormalization scheme at two-loop order is discussed in Section IV which completes the analytic aspect of the computation. Our results are presented in Section V which contains the form factor plots for all momenta in comparison to several lattice data sets. These have been compiled for different pion masses. Therefore the discussion of Section V centres on the error analysis for relating two loop results to data. After concluding remarks in Section VI there are four Appendices. The first illustrates all the graphs we have computed while the next discusses finer aspects of the two loop renormalization group flow. These ideas are illustrated in a third appendix using the simple case of the minimal subtraction scheme which we used as benchmark before implementing the Infrared Safe

renormalization scheme and which could also serve as a pedagogical introduction to two-loop running. The final appendix gathers next-to-leading order UV and IR asymptotic expansions of the various anomalous dimensions used in the present work.

II. THE CURCI-FERRARI MODEL

We turn to more specific aspects of our study and discuss the necessary background to the Curci-Ferrari model. In Ref. [17] the model was considered for an arbitrary covariant gauge parameter which featured a mass for the Faddeev-Popov ghosts as well as one for the gluons. However as the former depends linearly on the gauge parameter, the ghost mass vanishes in the Landau gauge limit on which we focus in this work. This is not unconnected with the massless longitudinal mode of the gluon.

A. Generalities

In the Landau gauge limit, the Euclidean CF Lagrangian density in the presence of N_f degenerate quark flavors (in the fundamental representation of the color group) reads

$$\mathcal{L} = \frac{1}{4} F_{\mu\nu}^a F_{\mu\nu}^a + i h^a \partial_\mu A_\mu^a + \partial_\mu \bar{c}^a (D_\mu c)^a$$
$$+ \frac{1}{2} m^2 (A_\mu^a)^2 + \sum_{i=1}^{N_f} \bar{\psi}_i (\slashed{D} + M) \psi_i \,, \qquad (1)$$

where $F_{\mu\nu}^a \equiv \partial_\mu A_\nu^a - \partial_\nu A_\mu^a + g f^{abc} A_\mu^b A_\nu^c$ is the field-strength tensor, h^a a Nakanishi-Lautrup field, $(c^a, \bar{c}^a)$ a pair of ghost and antighost fields, and $(\psi_i, \bar{\psi}_i)$ a pair of quark and antiquark fields for each flavor i. The covariant derivatives in the adjoint (ϕ) and fundamental (ψ) representations read respectively

$$(D_\mu \phi)^a \equiv \partial_\mu \phi^a + g f^{abc} A_\mu^b \phi^c, \qquad (2)$$
$$\mathcal{D}_\mu \psi \equiv \partial_\mu \psi - i g A_\mu^a t^a \psi \,, \qquad (3)$$

with f^{abc} the structure constants of the SU(N) gauge group and t^a the generators of the corresponding Lie algebra, normalized such that $\mathrm{tr}(t^a t^b) = \delta^{ab}/2$. The parameters g, m and M denote respectively the bare coupling constant, bare gluon mass and bare quark mass.

In what follows, we choose a Euclidean convention for the Dirac matrices, such that $\{\gamma_\mu, \gamma_\nu\} = 2\delta_{\mu\nu} 1$, with 1 the identity matrix in spinor space. The Dirac contraction $\slashed{D} \equiv \gamma_\mu \mathcal{D}_\mu$ is defined in terms of those Euclidean matrices. The formulas to be derived below are valid for an arbitrary number of colors and an arbitrary number of degenerate quark flavors (in the Landau gauge), but we shall restrict the comparison to the lattice data to the case of three colors and two degenerate flavors.

The model is regularized by working in $d = 4 - 2\epsilon$ dimensions. This allows us to take full advantage of the symmetries of the model, in particular the BRST symmetry mentioned above. These symmetries, together with the fact that the tree-level gluon propagator of the model is transverse and decreases with two powers of the momentum, ensure the renormalizability of the model. Renormalization proceeds along the usual lines. One first rescales the bare fields and bare parameters in terms of their renormalized counterparts. Denoting the bare quantities that appear in the action (1) with a subscript B, this step writes

$$A_B^{a\,\mu} = \sqrt{Z_A}\,A^{a\,\mu}, \;\; c_B^a = \sqrt{Z_c}\,c^a, \;\; \bar{c}_B^a = \sqrt{Z_c}\,\bar{c}^a,$$
$$\psi_B = \sqrt{Z_\psi}\,\psi, \;\; \bar{\psi}_B = \sqrt{Z_\psi}\,\bar{\psi}, \tag{4}$$

and

$$g_B = Z_g\,g, \quad m_B^2 = Z_{m^2}\,m^2, \quad M_B = Z_M M. \tag{5}$$

Then, the divergences present in the n-point functions of the model are absorbed in the various renormalization factors Z_X with $X \in \{A, c, \bar{c}, \psi, \bar{\psi}, g, m^2, M\}$ and the finite parts of these factors are fixed via a choice of renormalization scheme. In this work, we consider the so-called Infrared-safe renormalization scheme whose definition in terms renormalization conditions is reviewed below together with its main properties.

Let us recall here that, in dimensional regularization, the bare coupling acquires the mass dimension ϵ, which it is usually convenient to make explicit by introducing a scale. In this article, we denote this scale as Λ in such a way that the bare and renormalized couplings in (5) are rescaled as $g_B \to \Lambda^\epsilon g_B$ and $g \to \Lambda^\epsilon g$ respectively. The reason for this unusual choice is that this scale has a priori nothing to do with the renormalization scale μ that is introduced via the renormalization conditions. The scale Λ is in fact a scale associated with the regularization procedure, and, as such, the renormalized quantities do not depend on its choice in the continuum limit (corresponding to $\epsilon \to 0$) while they depend in general on the renormalization scale μ. We shall illustrate this below when evaluating the anomalous dimensions and the beta functions in the IR-safe scheme. We will also see that, in intermediate computational steps, that is prior to taking the continuum limit, it is convenient to keep the two scales Λ and μ independent of each other.[2]

B. Two-point functions

Our focus in this article is on the two-point functions of the model. These are obtained by inverting the second field derivative of the effective action $\Gamma[A, ih, c, \bar{c}, \psi, \bar{\psi}]$. In the ghost sector, this second derivative will be written as

$$\Gamma^{(2)}_{c^a \bar{c}^b}(k) \equiv \delta^{ab}\Gamma(k). \tag{6}$$

Similarly, in the gluon and quark sectors, we shall use the notation

$$\Gamma^{(2)}_{A_\mu^a A_\nu^b}(k) \equiv \delta^{ab}\left(P_{\mu\nu}^\perp(k)\Gamma^\perp(k) + P_{\mu\nu}^\parallel(k)\Gamma^\parallel(k)\right) \tag{7}$$

and

$$\Gamma^{(2)}_{\psi\bar{\psi}}(k) \equiv -i\slashed{k}\,\Gamma^\gamma(k) + \mathbb{1}\,\Gamma^1(k), \tag{8}$$

where

$$P_{\mu\nu}^\perp(k) \equiv \delta_{\mu\nu} - \frac{k_\mu k_\nu}{k^2} \quad \text{and} \quad P_{\mu\nu}^\parallel(k) \equiv \frac{k_\mu k_\nu}{k^2} \tag{9}$$

are the transverse and longitudinal projectors.

The ghost propagator is obtained as $G_{\text{gh}}(k) \equiv 1/\Gamma(k)$. From the derivative nature of the ghost-antighost-gluon tree-level vertex and the transverse nature of the tree-level gluon propagator, it is easily argued that $\Gamma(k)$ vanishes at least as k^2 in the limit $k \to 0$.[3] It is then convenient to define the ghost dressing function

$$F(k) \equiv k^2 G_{\text{gh}}(k) = k^2/\Gamma(k). \tag{10}$$

As for the gluon propagator, it is obtained by first inverting the second derivative of the effective action in the A/ih-sector and then restricting the so-obtained inverse to the A-sector. The ih-sector cannot be disregarded because it couples to the A-sector. However, since the ih-dependent part of the action is not renormalized [25], one is led to the inversion of the following matrix

$$\begin{pmatrix} P_{\mu\nu}^\perp(k)\Gamma^\perp(k) + P_{\mu\nu}^\parallel(k)\Gamma^\parallel(k) & ik_\mu \\ -ik_\nu & 0 \end{pmatrix}. \tag{11}$$

The inverse is easily found to be

$$\begin{pmatrix} P_{\mu\nu}^\perp(k)/\Gamma^\perp(k) & -ik_\mu/k^2 \\ ik_\nu/k^2 & \Gamma^\parallel(k)/k^2 \end{pmatrix}, \tag{12}$$

from which it follows that the gluon propagator is transverse, $P_{\mu\nu}^\perp(k)G(k)$, with $G(k) = 1/\Gamma^\perp(k)$. By analogy with the ghost sector, and despite the fact that $\Gamma^\perp(k)$

---

does not vanish as $k \to 0$, it is customary to introduce a gluon dressing function

$$D(k) \equiv k^2 G(k) = k^2 / \Gamma^{\perp}(k) \,. \qquad (13)$$

Finally, the quark propagator is obtained by inverting $\Gamma^{(2)}_{\psi\bar{\psi}}(k)$. Multiplying Eq. (8) by $i\slashed{k}\,\Gamma^{\gamma}(k) + 1\,\Gamma^1(k)$ and owing to the property $\slashed{k}^2 = k^2$, one finds the propagator

$$S(k) = \frac{i\slashed{k}\,\Gamma^{\gamma}(k) + 1\,\Gamma^1(k)}{k^2(\Gamma^{\gamma}(k))^2 + (\Gamma^1(k))^2} \,. \qquad (14)$$

It is customary to rewrite this as

$$S(k) = Z(k) \frac{i\slashed{k} + 1 M(k)}{k^2 + M^2(k)} \,, \qquad (15)$$

with

$$Z(k) \equiv 1/\Gamma^{\gamma}(k) \quad \text{and} \quad M(k) \equiv \Gamma^1(k)/\Gamma^{\gamma}(k) \,. \qquad (16)$$

The benefit of this rewriting is that $M(k)$ appears as the ratio of two tensor components of the same two-point function and, as such, is a finite, renormalization group invariant quantity, known as the quark mass function. As for the function $Z(k)$, we shall refer to it as the quark dressing function.

Although we shall not be dealing directly with three-point vertices in this work, let us mention here that a similar argument to the one used for the ghost propagator leads to the conclusion that loop corrections to the ghost-antighost-gluon vertex vanish in the limit of vanishing ghost momentum $k \to 0$:

$$\Gamma^{(3)}_{c^a A^b_\mu \bar{c}^c}(0, l, h) = -i f^{abc} g_B \Lambda^\epsilon h_\mu \,. \qquad (17)$$

This is Taylor's non-renormalization theorem in the CF model [25, 40, 54–57]. Another such theorem holds for the combination $\Gamma^{\parallel}(k) F^{-1}(k)$ which is related to the bare gluon mass via the Slavnov-Taylor identity [25]:

$$\Gamma^{\parallel}(k) F^{-1}(k) = m_B^2 \,. \qquad (18)$$

Upon renormalization, the two identities (17) and (18) constrain the combinations $Z_g \sqrt{Z_A} Z_c$ and $Z_{m^2} Z_A Z_c$ of renormalization factors to remain finite. These constraints are fully exploited within the Infrared-safe renormalization scheme which we now review.

C. Infrared safe renormalization scheme

The Infrared safe (or IR-safe in short) renormalization scheme is defined by extending the relations between the divergent parts of the renormalization factors Z_g, Z_{m^2}, Z_A and Z_c discussed in the previous section so as to include their finite parts. One then requires that

$$Z_g \sqrt{Z_A} Z_c = 1 \,, \quad Z_{m^2} Z_A Z_c = 1 \,. \qquad (19)$$

The benefit of these conditions is that they give access to Z_g and Z_{m^2} solely in terms of Z_A and Z_c. The latter are fixed by requiring that the renormalized ghost and gluon two-point functions (which depend both on the external momentum k and on the renormalization scale μ) satisfy the conditions

$$\Gamma(k = \mu; \mu) = 1 \,, \quad \Gamma^{\perp}(k = \mu; \mu) = \mu^2 + m^2(\mu) \,. \quad (20)$$

As for the quark renormalization factors Z_ψ and Z_M they are fixed by imposing the conditions

$$\Gamma^{\gamma}(k = \mu; \mu) = 1 \,, \quad \Gamma^1(k = \mu; \mu) = M(\mu) \,. \qquad (21)$$

Here, we are deliberately using the same notation for the renormalized mass and for the quark mass function defined in the previous section. In a generic renormalization scheme, these two functions do not need to coincide. In the present scheme however, they do coincide because the bare components $\Gamma^{\gamma}(k)$ and $\Gamma^1(k)$ renormalize identically, so that one has

$$\frac{\Gamma^1(k)}{\Gamma^{\gamma}(k)} = \frac{\Gamma^1(k; \mu)}{\Gamma^{\gamma}(k; \mu)} = \frac{\Gamma^1(k; k)}{\Gamma^{\gamma}(k; k)} \,, \qquad (22)$$

with the left-hand side corresponding to the quark-mass function and the right-hand side corresponding to the renormalized mass in the present scheme and at scale $\mu = k$.

Once all the renormalization factors are known from (19)-(21), one can determine the various anomalous dimensions and beta functions. These are necessary in order to obtain a controlled perturbative description of the various propagators, in those cases where large logarithms (associated with large separations of scales) would invalidate the use of a naïve perturbative expansion. For the moment we skip all details concerning the practical implementation of the renormalization group (RG) as they will be recalled in full detail when considering the RG flow at two-loop order in Sec. IV.

One of the main benefits of the IR-safe renormalization scheme is that it features renormalization group trajectories that are free of any Landau singularity and along which the running coupling remains moderate, allowing for a perturbative investigation of the CF model over all scales.[4] Based on these properties, the one-loop ghost, gluon, and quark dressing functions, as well as the quark mass function were evaluated in Ref. [1] within the IR-safe renormalization scheme for an arbitrary number of colors, degenerate flavors and dimensions, and compared with lattice data in the particular case of $d = 4$ and $N = 3$, for $N_f = 2$, $2 + 1$ and $2 + 1 + 1$ flavors, [50–53]. Let us now briefly review these results.

_____

[4] Other useful features of the IR-safe renormalization scheme will be reviewed in Sec. IV.

D. Summary of one-loop results

The one-loop CF results for the ghost and gluon dressing functions were found to reproduce the unquenched lattice data with high precision. Moreover, the results for these two functions appeared to be rather insensitive to the choice of the renormalized quark mass at the initialization of the RG flow. One of the goals of this article is to investigate whether these results improve further upon the inclusion of higher order (two-loop) corrections. This would support the perturbative paradigm, at least for these quantities.

The situation in the quark sector is more delicate. In Ref. [1], the quark mass function was correctly reproduced, although not as accurately as for the ghost and gluon dressing functions. On the other hand, it is well known that perturbation theory cannot capture the spontaneous breaking of chiral symmetry. Therefore, we should expect the quality of the perturbative CF results to decrease as one tries to compare with lattice data closer to the chiral limit (which were not available at the time the analysis in Ref. [1] was performed). This means that, in this regime, one cannot provide an equally good description of the quark mass function over the whole range of momenta. If one insists in reproducing the low momentum range, there will be inevitably an offset in the ultraviolet range which grows as the chiral limit is approached, and, equivalently, if one insists in reproducing the ultraviolet range, the quark mass function will not develop enough strength in the infrared to generate the correct mass.

It should be stressed that the CF model is not to blame here, but rather the use of the perturbative expansion in the light quark regime. Indeed, in this range of quark masses, the quark-gluon coupling is a few times larger than the pure gauge coupling, jeopardizing the use of a purely perturbative approach. As recalled in the Introduction, a way to cope with this limitation while remaining within the CF model, is to consider the Rainbow-Improved (RI) expansion, a double expansion in powers of the pure gauge coupling (which remains perturbative) and of the inverse number of colors. This systematic computational scheme has been considered at leading and next-to-leading order in Refs. [41, 42] where it has been shown to capture the spontaneous breaking of chiral symmetry while providing a good simultaneous account of the ghost and gluon dressing functions and the quark mass function.

The RI expansion lies however beyond the strict scope of the present paper which aims instead at investigating to which extent the perturbative CF model up to two-loop order can describe the various two-point functions, in particular in the case of the most chiral data available to date [52]. This analysis is interesting in its own right, even when including the quark mass function in the fit. Of course, as we just explained, we may expect some tension in the quark mass function but it is interesting to see whether this tension is amplified or reduced upon

the inclusion of higher order corrections, and also how it impact on the other functions. For completeness, we shall also consider a partial fit of all the two-point functions that we believe have a perturbative description within the CF models, that is excluding the quark mass function but including the quark dressing function.

That the quark dressing function $Z(k)$ admits a perturbative description is not obvious from the results of Ref. [1]. In this reference, the one-loop prediction for this function in the CF model was seen not to reproduce the lattice data, not even qualitatively as the function was found to have the wrong monotonicity/convexity. Here, however, the mismatch cannot be attributed to a too large quark-gluon coupling since the RI resummation does not help in this respect [41, 42] and the mismatch occurs also for large quark masses. In fact, the one-loop contribution to $Z(k)$ turns out to be unusually small and even vanishes in the limit of zero gluon mass, a well known result in the Landau gauge. This indicates that two-loop corrections represent an important contribution to $Z(k)$ and should not be neglected,[5] before any judgement on the validity of perturbation theory for this quantity. In Ref. [1], an estimate of the two-loop corrections to $Z(k)$ was proposed that hinted to a solution of the monotonicity/convexity problem with the inclusion of these contributions. This provides a further motivation for evaluating the two-loop corrections to the various two-point functions, and, by slightly anticipating the results that will be presented below, we can already state here that $Z(k)$ admits an accurate perturbative description at two-loop order within the CF model.

Let us end this review of existing one-loop results by mentioning that the one-loop quark-gluon vertex has also been evaluated in Ref. [26]. The lattice data for this function are well reproduced by the leading order CF approximation. In particular, as is already the case for the ghost dressing function, the one-loop diagrams contributing to this vertex are the same in both the quenched and unquenched cases since no quark loops are involved. Therefore, the dynamical quarks contribute to these functions only through the running of the coupling and the masses, and the effect is small as compared to the quenched case. An estimate of the two-loop corrections for this function is left for a future investigation. For now, we concentrate on the evaluation of the two-loop corrections to the various two-point functions of the CF model, which we describe in the next section. The implementation of the renormalization group at two-loop order in the IR-safe scheme will be dealt with in Sec. IV.

---

[5] They become the leading order corrections in the zero gluon mass limit.

III.   UNQUENCHED TWO-POINT FUNCTIONS AT TWO-LOOP ORDER

We devote this section to the details of how the two loop corrections to the Landau gauge gluon, ghost and quark two-point functions are evaluated in the presence of non-zero gluon and quark masses. Once the two-point functions are determined as functions of the bare parameters, we carry out the renormalization at two-loop order. Aside from being necessary for our ultimate goal, it provides an intermediate check on our original set-up. Additional cross-checks will also be discussed. Some of these entail checking that previous results, such as the case when quarks are massless, correctly emerge in the limit $M \to 0$ for example.

A.   Notation

Since we shall often refer simultaneously to the various two-point functions Γ, $\Gamma^{\perp}$, $\Gamma^{\parallel}$, Γ^{γ}, Γ^{1} introduced in the previous section, it will be convenient to denote them generically as Γ^{C} with $C \in \{\emptyset, \perp, \parallel, \gamma, 1\}$ and where the empty set $\emptyset$ is used to refer to the ghost component $\Gamma(k)$. Moreover, we write

$$\begin{aligned}
\Gamma^{C}(k) = {} & \Gamma_{0}^{C}(k^{2}, m_{B}^{2}, M_{B}) \\
& + \lambda_{B}\, \Gamma_{1}^{C}(k^{2}, m_{B}^{2}, M_{B}) \\
& + \lambda_{B}^{2}\, \Gamma_{2}^{C}(k^{2}, m_{B}^{2}, M_{B})\,,
\end{aligned} \tag{23}$$

where $\Gamma_{n}^{C}(k^{2}, m_{B}^{2}, M_{B})$ represents the sum of n-loop Feynman diagrams contributing to $\Gamma^{C}(k)$. For convenience, we have factored out λ_{B}^{n}, with

$$\lambda_{B} \equiv \frac{g_{B}^{2}N}{16\pi^{2}}\,, \tag{24}$$

in front of $\Gamma_{n}^{C}(k^{2}, m_{B}^{2}, M_{B})$. In practice, this means that, in computing Feynman diagrams contributing to $\Gamma_{n}^{C}(k^{2}, m_{B}^{2}, M_{B})$, the d-dimensional momentum integrals are replaced by

$$\int \frac{d^{d}p}{(2\pi)^{d}} \to \int_{p} \equiv 16\pi^{2}\Lambda^{2\epsilon} \int \frac{d^{d}p}{(2\pi)^{d}}\,, \tag{25}$$

and the color factors are all systematically divided by N^{n}.

The tree-level contributions $\Gamma_{0}^{C}(k^{2}, m_{B}^{2}, M_{B})$ are linear in any of their arguments. More precisely, we have

$$\Gamma_{0} = k^{2}\,,\ \Gamma_{0}^{\perp} = k^{2} + m_{B}^{2}\,,\ \Gamma_{0}^{\parallel} = m_{B}^{2}\,,\ \Gamma_{0}^{\gamma} = 1\,,\ \Gamma_{0}^{1} = M_{B}\,.$$

The one-loop contributions $\Gamma_{1}^{C}(k^{2}, m_{B}^{2}, M_{B})$ have been systematically evaluated in Ref. [1] and expressed in terms of the two one-loop master integrals

$$A_{m_{a}} \equiv \int_{p} G_{m_{a}}(p)\,, \tag{26}$$

$$B_{m_{a}m_{b}}(k^{2}) \equiv \int_{p} G_{m_{a}}(p)G_{m_{b}}(p+k)\,. \tag{27}$$

As for the two-loop contributions $\Gamma_{2}^{C}(k^{2}, m_{B}^{2}, M_{B})$, as we now explain, they can be systematically reduced to the evaluation of the two-loop master integrals

$$\begin{aligned}
& S_{m_{a}m_{b}m_{c}}(k^{2}) \\
& \equiv \int_{p} G_{m_{a}}(p)B_{m_{b}m_{c}}((p+k)^{2})\,,
\end{aligned} \tag{28}$$

$$\begin{aligned}
& U_{m_{a}m_{b}m_{c}m_{d}}(k^{2}) \\
& \equiv \int_{p} G_{m_{b}}(p)G_{m_{a}}(p+k)B_{m_{c}m_{d}}(p^{2})\,,
\end{aligned} \tag{29}$$

$$\begin{aligned}
& M_{m_{a}m_{b}m_{c}m_{d}m_{e}}(k^{2}) \\
& \equiv \int_{p} G_{m_{a}}(p)G_{m_{c}}(p+k) \\
& \quad \times \int_{q} G_{m_{b}}(q)G_{m_{d}}(q+k)G_{m_{e}}(q-p)\,,
\end{aligned} \tag{30}$$

which can then be evaluated numerically using the TSIL package [58].

B.   Reduction to master integrals

One starts with the generation of the two-loop Feynman graphs contributing to each of the two-point functions. This is achieved using the FORTRAN based QGRAF package, [59]. There are 23, 7 and 7 graphs at two loops for the gluon, ghost and quark two-point functions respectively compared with 4, 1 and 1 graphs respectively at one loop. These are illustrated in App. A. In generating the graphs we have included snail topologies. Ordinarily, such graphs are excluded when there is no gluon mass since they would vanish in dimensional regularization in this particular case.

Once the graphs have been generated for each two-point function, the next stage, after appending colour and Lorentz indices, is to write each Green's function in terms of scalar integrals. The reason for this resides in the techniques we use to evaluate the large set of integrals. The path to the scalar integrals proceeds in several steps. First, for the gluon and quark two-point functions we have to project out the transverse and longitudinal components in the former case, and in the latter case we have to isolate the contributions proportional to $\not{k}$ and 1, see Eqs. (7) and (8). Of course, no projection is necessary for the ghost two-point function.

While this converts tensor Feynman integrals with no free Lorentz or spinor indices into scalar ones, the resultant integrals still contain scalar products of loop and external momenta. To two-loop order, all such scalar products can be rewritten in terms of the squared length of the propagator momenta, using for instance

$$k \cdot p = \frac{1}{2}\left[k^{2} + p^{2} - (k-p)^{2}\right] \tag{31}$$

for the massless case, where p is a loop momentum. When a non-zero mass m is present one merely makes the extra

replacement

$$(k - p)^2 = [(k - p)^2 + m^2] - m^2 \qquad (32)$$

for the appropriate propagator. This produces integrals with no scalar products but rational polynomials of the propagators. It is in this representation that each Feynman integral of the large set of integrals appearing in the two-point functions has to be written in order to imple-

ment the standard integration technique now widely used in multi-loop computations. This is the Laporta algorithm, [60], which is based on a systematic use of integration by parts. In particular, we used the REDUZE implementation, [61, 62], written in C++ with GiNaC, [63], as the core algebra foundation component. To organize the tedious algebra associated with writing the integrals contributing to a Green's function, we have employed the symbolic manipulation language FORM, [64, 65].
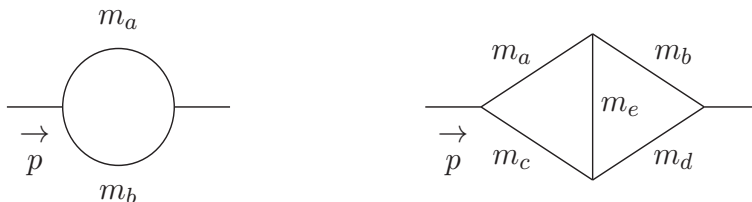

FIG. 1. Graphical representations of $I_{1ab}(n_1, n_2)$ and $I_{abcde}(n_1, n_2, n_3, n_4, n_5)$ defined in (33) and (34).

The consequence is that the two-loop integrals can all be written in terms of two basic integrals which are a one-loop one and a two-loop one. The one loop one is

$$I_{1ab}(n_1, n_2) = \int_p \frac{1}{[p^2 + m_a^2]^{n_1}[(p - k)^2 + m_b^2]^{n_2}} \,, \quad (33)$$

where n_i are integers both positive and negative. We use m_a and m_b as generic masses which can both take values from the set $\{0, m, M\}$ of the three possible masses that will concern us here. The two-loop core integral is

$$I_{abcde}(n_1, n_2, n_3, n_4, n_5) = \int_{pq} \frac{1}{[p^2 + m_a^2]^{n_1}[q^2 + m_b^2]^{n_2}[(p - k)^2 + m_c^2]^{n_3}[(q - k)^2 + m_d^2]^{n_4}[(p - q)^2 + m_e^2]^{n_5}} \quad (34)$$

in the same notation as (33) which extends that used in Ref. [37]. Moreover this syntax is the one we used for defining the integral families of the Laporta algorithm. The two integrals have the graphical representations given in Fig. 1. While (34) is the most general massive two-loop self-energy structure, we will only be concerned with two non-zero masses. To understand the types of integrals that can actually appear in the evaluation of the two-point functions, we provide two examples for each of the gluon and quark two-point functions in Fig. 2. The respective labels shown underneath each

graph indicate one of the set of integrals of (34) that can arise. However for lines involving gluons some of the propagators that emerge will be massless. So in addition to I_{ababb} the structures I_{0babb}, I_{ab0bb} and I_{0b0bb} will be present. When 0 appears in the label it indicates a massless propagator with the convention that $m_0 \equiv 0$. So for the other graphs I_{bbbb0} will be present in the other gluon self-energy diagram. For the two quark self-energy graphs I_{0bbab}, I_{abb0b} and I_{0bb0b} will also occur in addition to I_{abbab}. For that labelled I_{aabba} there are seven other contributions which are I_{aabb0}, I_{a0bba}, I_{0abba}, I_{00bba}, I_{0abb0}, I_{a0bb0} and I_{00bb0}.

While the actual non-zero masses in our computations are m and M we use m_a and m_b for the inte-
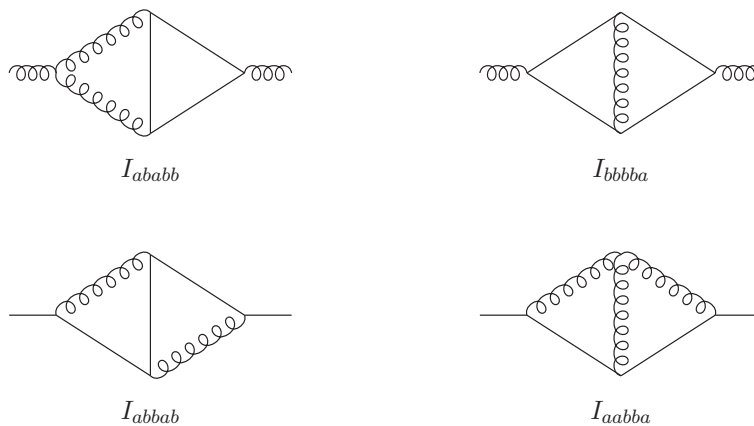
FIG. 2. Graphs in gluon and quark 2-point functions containing the labelled integrals as examples. Gluon propagators are represented by curly lines while quarks are denoted by straight ones.

gral definitions since in the process to write each Green's function in terms of scalar integrals, other topologies are present at two loops which are illustrated in Fig. 3. For example, each graph is contained in I_{abcde} through $I_{abcde}(0, n_2, 0, n_4, n_5)$ for the sunset diagram and $I_{abcde}(n_1, n_2, 0, n_4, n_5)$ for the graph with four propagators. The sunset integral $I_{aaaab}(0, n_2, 0, n_4, n_5)$ that arises in the graph labelled I_{abbab} in Fig. 2 is equivalent to $I_{ababa}(0, n_2, 0, n_4, n_5)$ which occurs in that labelled by I_{ababb} of the same figure. One can see this by noting that if the propagator is absent then the argument of the function corresponding to it is zero. So the respective mass label can be anything or 0, a or b in this case. In addition, the sunset topology has a sixfold permutation symmetry that ensures the equality. The outcome is that the labels a and b on the general two loop integral in the two mass case could correspond to either quark or gluon mass or vice versa depending on the Green's function and ultimate topology. Therefore in applying the Laporta algorithm we have built the system of integration by parts equations for a generic set of mass configurations based on arbitrary masses m_a and m_b. Therefore in (34) the elements of the two loop integral family is given by allowing each of the labels in the integral to be one of the set $\{0, m_a, m_b\}$. While this would produce 3^5 core integrals the actual number is fewer due to using rotational symmetry such as

$$I_{0aaba}(n_1, n_2, n_3, n_4, n_5) = I_{a0baa}(n_2, n_1, n_4, n_3, n_5)$$
$$= I_{baa0a}(n_4, n_3, n_2, n_1, n_5) \quad (35)$$

and similar relations for others with related label patterns. Equally if the exponent of a massive propagator is zero then we relabel the corresponding index on $I_{abcde}(n_1, n_2, n_3, n_4, n_5)$ as 0 by default.

Dwelling on this notational aspect of the calculation is important since it is in a language that can be coded for the REDUZE version of the Laporta algorithm. For instance, we have used the labels in (33) and (34) to define

FIG. 3. Additional two loop topologies that arise in each 2-point function.

the integral families for the application of the REDUZE package. There are not 3^5 cases in total since we reduce the number by using the separate left-right and up-down symmetries of the two loop graph of Fig. 1. This substantially lowers the number of cases. An example of this was given in (35). The result of applying the Laporta algorithm, [60], is to reduce the evaluation of all the graphs and integrals in the two-point functions to a set of master integrals which is significantly smaller than the original input set. However the coefficients of each master are functions of the two masses, the external momentum and the spacetime dimension d. The presence of two non-zero masses means the set of master integrals is larger than that for the single scale problem of Ref. [37]. Given this, we follow the same approach in the sense we choose a basis for the masters that tallies with the integrals of the TSIL package [58] which we use extensively. It evaluates two loop self-energy integrals with non-zero masses numerically and allows us to determine the behaviour of the Green's function over all momenta. More specifically the mapping to the master integrals given above (which are the ones defined in the TSIL package) is

$$I_{1a0}(1,0) = A_{m_a} \;,\; I_{1ab}(1,1) = B_{m_a m_b} \quad (36)$$

at one loop. At two loops we have

$$I_{ab00c}(1,1,0,0,1) = I_{m_a m_b m_c}$$
$$I_{0ab0c}(0,1,1,0,1) = S_{m_a m_b m_c}$$
$$I_{abc0d}(1,1,1,0,1) = U_{m_c m_a m_b m_d}$$
$$I_{abcde}(1,1,1,1,1) = M_{m_a m_b m_c m_d m_e} \;, \quad (37)$$

where the first mapping corresponds to the two loop vacuum bubble $I_{m_a m_b m_c} = S_{m_a m_b m_c}(k^2 = 0)$. We also encounter

$$I_{0ab0c}(0,2,1,0,1) = T_{m_a m_b m_c}$$
$$I_{abc0d}(2,1,1,0,1) = V_{m_c m_a m_b m_d} \,, \qquad (38)$$

with $T_{m_a m_b m_c} = -\partial S_{m_a m_b m_c}/\partial m_a^2$ and $V_{m_c m_a m_b m_d} = -\partial U_{m_c m_a m_b m_d}/\partial m_a^2$ but we note that these mass derivatives can be expressed in terms of the other master integrals. The remaining masters are the product of one loop masters since

$$I_{ab000}(1,1,0,0,0) = I_{1a0}(1,0)I_{1b0}(1,0)$$
$$I_{ab000}(1,1,1,0,0) = I_{1a0}(1,1)I_{1b0}(1,0)$$
$$I_{ab0c0}(1,1,0,1,0) = I_{1a0}(1,0)I_{1bc}(1,1)$$
$$I_{abcd0}(1,1,1,1,0) = I_{1ac}(1,1)I_{1bd}(1,1) \,. \qquad (39)$$

We note that the electronic version of each of our two-point functions can be found in Ref. [67].

C. Renormalization

Once written in terms of the master integrals, it is fairly easy to isolate the UV divergences in each two-point function (23), the renormalization of which proceeds along the usual lines. First, one rescales the corresponding function by the appropriate factor, $\Gamma^C \to Z_C \Gamma^C$, with

$$Z_{\emptyset} = Z_c \,, \quad Z_{\perp} = Z_{\parallel} = Z_A \,, \quad Z_{\gamma} = Z_1 = Z_{\psi} \,. \quad (40)$$

Next, one expresses the bare parameters in terms of renormalized ones, $m_B^2 = Z_{m^2}m^2$ and $\lambda_B = Z_\lambda \lambda$. Finally, one writes each renormalization factor Z as $Z = 1 + \delta Z$ with δZ a formal series in powers of the renormalized coupling λ, which one expands to the relevant order. At one-loop order for instance, the renormalized two-point functions read

$$\Gamma^C(k) = \Gamma_0^C(k^2, m^2, M) + \lambda \, \Gamma_1^C(k^2, m^2, M)$$
$$+ \mathcal{R}^{11} \Gamma_0^C(k^2, m^2, M) \,, \qquad (41)$$

where $\mathcal{R}$ is the operator

$$\mathcal{R} \equiv \delta Z_C + \delta Z_{m^2}m^2\frac{\partial}{\partial m^2} + \delta Z_M M\frac{\partial}{\partial M} \,, \qquad (42)$$

and $\mathcal{R}^{\mathrm{nl}}$ refers to its n-loop truncation, obtained by truncating the counterterms accordingly. It should be mentioned that, because the tree-level contribution $\Gamma_0^C(k^2, m^2, M) = u^C k^2 + v^C m^2 + w^C M$ is linear with respect to any of its arguments (with u^C, v^C, w^C equal to 0 or 1), the action of the operator $\mathcal{R}$ on $\Gamma_0^C(k^2, m^2, M)$ writes, at any order,

$$u^C \delta Z_C k^2 + v^C(\delta Z_C + \delta Z_{m^2})m^2 + w^C(\delta Z_C + \delta Z_M)M \,. \qquad (43)$$

This applies in particular to the term in the second line of Eq. (41). Therefore, each counterterm appearing in this term allows one to absorb the one-loop divergences that are present in the first line of (41) and that are proportional to k^2, m^2 and M. More precisely, writing the one-loop counterterms δZ_X^{11} with $X \in \{C, m^2, M\}$ as

$$\delta Z_X^{11} = \lambda \frac{z_{X,1}}{\epsilon} \,, \qquad (44)$$

with $z_{X,1} = z_{X,11} + \epsilon z_{X,10}$, the elimination of divergences amounts to the proper adjustment of the factors $z_{X,11}$. We mention that these factors are universal numbers that do not depend on the considered renormalization scheme. We checked that the values we obtained agree with the well known results, see for instance [68, 69]. In particular, we find that $z_{\psi,11} = 0$, in line with the fact that the one-loop corrections to $Z(k)$ vanish in the limit of a massless gluon, and, therefore, that they are UV finite for a non-zero m. On the other hand, the factors $z_{X,10}$ (which produce finite contributions to the one-loop counterterms) have to do with the scheme specification. They can depend on the scales Λ and μ as well as on the various masses present in the problem and will enter directly the anomalous dimensions and beta functions which we discuss in Sec. IV.

Similarly, at two-loop order, one finds

$$\Gamma^C(k) = \Gamma_0^C(k^2, m^2, M) + \lambda \Gamma_1^C(k^2, m^2, M) + \lambda^2 \Gamma_2^C(k^2, m^2, M)$$
$$+ \lambda \left(\delta Z_\lambda^{11} + \mathcal{R}^{11}\right) \Gamma_1^C(k^2, m^2, M) + \mathcal{R}^{21} \Gamma_0^C(k^2, m^2, M) \,. \qquad (45)$$

The role of the first term in the second line of (45) is to absorb the subdivergences hidden in the first line. We mention that all the divergent parts of the counterterms appearing in this term have been determined in the previous step, with the exception of the one in δZ_λ^{11}. However, the latter can be easily determined from the fact that, after this divergent part is fixed, there should only remain

divergences that are proportional to k^2, m^2 and M, so that they can be absorbed in the second term of (45) which has again the form (43). The two-loop counterterms in this term can be written as

$$\delta Z_X^{21} = \lambda \frac{z_{X,1}}{\epsilon} + \lambda^2 \frac{z_{X,2}}{\epsilon^2} \,, \qquad (46)$$

where $z_{X,1}$ has already been determined at one-loop or-

der and $z_{X,2} = z_{X,22} + \epsilon z_{X,21} + \epsilon^2 z_{X,20}$. Again, the factors $z_{X,22}$ are pure constants that do not depend on the renormalization scheme, and we have checked that the values we obtained match known results [68, 69]. The factors $z_{X,21}$, even though they have also to do with divergences, are not universal and are impacted by the choice of scheme at one-loop order. Obviously, the factor $z_{X,20}$ is also impacted by the choice of scheme. It will enter the anomalous dimensions and beta functions at two-loop order, as we show in Sec. IV.

Before closing this section, let us make an important remark. Of course, the main purpose of eliminating the divergences is to obtain finite expressions for the two-point functions in the continuum limit $\epsilon \to 0$. In this respect, one should not forget certain terms that survive in this limit from cancellations of the form $\epsilon \times 1/\epsilon$. One important such contributions arises from ϵ^2 corrections to the factor $z_{X,1}$ in (46). In principle, when implementing a given renormalization scheme at one-loop order, the factor $z_{X,1}$ receives such a contribution and in fact any power of ϵ. Of course, when it comes to evaluating the one-loop order two-point functions in the continuum limit, these higher powers of ϵ are irrelevant. However, the ϵ^2 contribution to $z_{X,1}$ is not irrelevant in the first term of the second line of (45) because it produces a term of order ϵ^0 that persists in the continuum limit. In this term, one should take instead $z_{X,1} = z_{X,11} + \epsilon z_{X,10} + \epsilon^2 z_{X,1(-1)}$ where $z_{X,1(-1)}$ is determined by implementing the renormalization scheme at one-loop order and for a finite value of ϵ. For similar reasons, the factors $z_{X,1(-1)}$ also enter the anomalous dimension and beta functions at two-loop order, as we show in Sec. IV.

D.   Cross-checks

As a result of the reduction of the two-loop two-point functions, one obtains expressions in terms of master integrals multiplied by rational functions of k^2, m^2 and M^2. Since these expressions are rather lengthy, it is preferable to test them as much as possible before any serious practical application. In this section, we review the various tests that we used in order to cross-check our expressions.

We mention that all these tests can be performed prior to renormalization. On the other hand, the renormalization of the two-loop expressions represents a test in itself since the cancellation of subdivergences by the counterterms determined at one-loop occurs only if the diagrams are computed and combined correctly in order to generate the correct subdivergences, as we described in the previous section. Another test related to renormalization that we considered was to retrieve the correct renormalization factors in the minimal subtraction scheme. Although this is not the scheme we use eventually for our comparison to lattice data, it is useful in order to understand certain features in a simpler setting and we provide a self-contained discussion in App. C.

Let us just mention here that, in this scheme, one has $z_{X,10} = z_{X,1(-1)} = z_{X,20} = 0$ by definition. We checked that the values obtained for $z_{X,11}$, $z_{X,22}$ and $z_{X,21}$ correspond to the well known results of Ref. [68, 69].

We now describe our other tests in detail.

1.   Quenched limit

In Ref. [37], the ghost and gluon two-point functions were studied in the quenched limit. We have checked that our unquenched expressions for these functions lead to the expressions of that reference in the limit $N_f \to 0$.

2.   Ultraviolet behaviour

Based on the superficial degree of divergence of the diagrams contributing to each of the two-point functions, we expect the following large momentum behaviour to hold true from Weinberg's theorem, [70],

$$\lim_{k\to\infty} \frac{\Gamma(k)}{|k|^3} = 0, \quad \lim_{k\to\infty} \frac{\Gamma^\perp(k)}{|k|^3} = 0, \tag{47}$$

$$\lim_{k\to\infty} \frac{\Gamma^\gamma(k)}{|k|} = 0, \quad \text{and} \quad \lim_{k\to\infty} \frac{\Gamma^1(k)}{|k|} = 0. \tag{48}$$

One difficulty in checking this behavior is that they are not obeyed by all the terms that make the reduced expression of each two-point function. Rather, they emerge after certain cancellations occur between these terms. Since it is in general difficult to check these cancellations numerically, we resorted to an analytical check using UV asymptotic expansions of the various master integrals, which were derived through our own implementation of the algorithm described in Ref. [71]. An earlier version of this algorithm was already used in Ref. [37]. For the present investigation, we had to extend it to the case where two mass scales are present in the master integrals. At leading order, we obtain the expressions:

$$\frac{\Gamma(k)}{k^2} = 1 - \lambda \left[1 + \frac{3}{4} \ln\left(\frac{\mu^2}{k^2}\right) \right]$$
$$- \lambda^2 \left[\frac{1751}{192} - \frac{15}{16}\zeta(3) - \frac{95}{48}\frac{N_f}{N} \right.$$
$$+ \left(\frac{235}{48} - \frac{13}{12}\frac{N_f}{N} \right) \ln\left(\frac{\mu^2}{k^2}\right)$$
$$\left. + \left(\frac{35}{32} - \frac{1}{4}\frac{N_f}{N} \right) \ln\left(\frac{\mu^2}{k^2}\right)^2 \right]$$
$$+ \mathcal{O}\left(\frac{m^2}{k^2}, \frac{M^2}{k^2} \right), \tag{49}$$

$$\frac{\Gamma^\perp(k)}{k^2} = 1 - \lambda \left[\frac{97}{36} - \frac{10}{9}\frac{N_f}{N} \right.$$
$$\left. + \left(\frac{13}{6} - \frac{2}{3}\frac{N_f}{N} \right) \ln\left(\frac{\mu^2}{k^2} \right) \right]$$
$$- \lambda^2 \left[\frac{2381}{96} - \frac{59}{8}\frac{N_f}{N} - \frac{55}{6}\frac{C_F}{N}\frac{N_f}{N} \right.$$
$$- \zeta(3)\left(3 + 4\frac{N_f}{N} - 8\frac{C_F}{N}\frac{N_f}{N} \right)$$
$$+ \left(\frac{137}{12} - \frac{25}{6}\frac{N_f}{N} - 2\frac{C_F}{N}\frac{N_f}{N} \right) \ln\left(\frac{\mu^2}{k^2} \right)$$
$$\left. + \left(\frac{13}{8} - \frac{1}{2}\frac{N_f}{N} \right) \ln\left(\frac{\mu^2}{k^2} \right)^2 \right]$$
$$+ \mathcal{O}\left(\frac{m^2}{k^2}, \frac{M^2}{k^2} \right), \tag{50}$$

$$\Gamma^\gamma(k) = 1 + \lambda^2 \frac{C_F}{N} \left[\frac{41}{4} - 3\zeta(3) - \frac{5}{8}\frac{C_F}{N} - \frac{7}{4}\frac{N_f}{N} \right.$$
$$\left. + \left(\frac{25}{4} - \frac{3}{2}\frac{C_F}{N} - \frac{N_f}{N} \right) \ln\left(\frac{\mu^2}{k^2} \right) \right]$$
$$+ \mathcal{O}\left(\frac{m^2}{k^2}, \frac{M^2}{k^2} \right), \tag{51}$$

and

$$\frac{\Gamma^1(k)}{M} = 1 + \lambda\frac{C_F}{N} \left[4 + 3\ln\left(\frac{\mu^2}{k^2} \right) \right]$$
$$+ \lambda^2 \frac{C_F}{N} \left[\frac{1531}{24} + 13\frac{C_F}{N} - \frac{26}{3}\frac{N_f}{N} \right.$$
$$- \zeta(3)\left(21 - 12\frac{C_F}{N} \right)$$
$$+ \left(\frac{445}{12} + 12\frac{C_F}{N} - \frac{16}{3}\frac{N_f}{N} \right) \ln\left(\frac{\mu^2}{k^2} \right)$$
$$\left. + \left(\frac{11}{2} + \frac{9}{2}\frac{C_F}{N} - \frac{N_f}{N} \right) \ln\left(\frac{\mu^2}{k^2} \right)^2 \right]$$
$$+ \mathcal{O}\left(\frac{m^2}{k^2}, \frac{M^2}{k^2} \right), \tag{52}$$

which indeed verify (47) and (48). In the equations above, $C_F = (N^2 - 1)/(2N)$ denotes the fundamental SU(N) Casimir. We have also used that the adjoint Casimir is $C_A = N$. For the sake of simplicity, we provide the asymptotic behaviors as obtained in the minimal subtraction scheme. We could easily derive them in a generic renormalization scheme, in which case the corresponding expressions depend explicitly on $z_{X,10}$, $z_{X,1(-1)}$ and $z_{X,20}$. Let us also mention that the absence of terms of order λ in the leading order contribution of $\Gamma^\gamma(k)$ relates again to the fact that these terms cancel in the limit of a vanishing gluon mass.

We mention that Weinberg's theorem [70] implies also that $\lim_{k\to\infty} \Gamma^\parallel(k)/|k|^3 = 0$, but in fact, from the Slavnov-Taylor identity (18), we have a stronger constraint, namely $\lim_{k\to\infty} \Gamma^\parallel(k)/|k| = 0$. By plugging (23) into (18) and expanding up to the relevant order, we find

$$m_B^2 \Gamma_1 + k^2 \Gamma_1^\parallel = 0 \tag{53}$$

and

$$m_B^2 \Gamma_2 + k^2 \Gamma_2^\parallel + \Gamma_1 \Gamma_1^\parallel = 0. \tag{54}$$

We have checked that these identities hold true, thus confirming the Slavnov-Taylor identity (18) at two-loop order and the corresponding UV suppression of $\Gamma^\parallel(k)$ with respect to the naïve counting.

3. Infrared behaviour

In the opposite momentum range, we expect the two-point functions $\Gamma^C(k)$ to be regular. This is because, these functions are built out of Euclidean Feynman integrals and there are always enough massive propagators to regularize the $k \to 0$ limit. As we have already discussed, in the case of the ghost two-point function, $\Gamma(k)$ is not only regular in this limit, but vanishes at least as k^2.

Again, these expectations might be difficult to check numerically because they typically emerge as the result of cancellations between various terms in the reduced expressions for $\Gamma^C(k)$, which themselves do not behave accordingly. We then resorted to an analytical check that requires the expansion of the various master integrals in powers of k^2.

We first checked that the various master integrals that produce the wrongly behaving terms always involve enough massive propagators in such a way that the routing of k inside the integral can always be chosen to avoid massless propagators. In this situation, we can employ the strategy of Ref. [72] that leads to a regular expansion in powers of k^2 with coefficients given by the momentum independent master integrals A_{m_a} and $I_{m_a m_b m_c} \equiv S_{m_a m_b m_c}(k^2 = 0)$ and their mass derivatives. The latter mass derivatives can always be conveniently re-expressed in terms of A_{m_a} and $I_{m_a m_b m_c}$ using

$$\frac{\partial}{\partial m_a^2} A_{m_a} = (d/2 - 1)\frac{A_{m_a}}{m_a^2} \tag{55}$$

that follows from dimensional analysis and

$$\Delta_{m_a m_b m_c} \frac{\partial}{\partial m_c^2} I_{m_a m_b m_c}$$
$$= (d-3)(m_a^2 + m_b^2 - m_c^2) I_{m_a m_b m_c}$$
$$+ (d-2)\left[A_{m_a} A_{m_b} + \frac{m_a^2 - m_b^2 - m_c^2}{2m_c^2} A_{m_a} A_{m_c} \right.$$
$$\left. + \frac{m_b^2 - m_a^2 - m_c^2}{2m_c^2} A_{m_b} A_{m_c} \right], \tag{56}$$

with

$$\Delta_{m_a m_b m_c} = m_a^4 + m_b^4 + m_c^4$$
$$- 2\left(m_a^2 m_b^2 + m_b^2 m_c^2 + m_c^2 m_a^2\right), \quad (57)$$

that follows from integration by parts techniques [72, 73]. In this way, the coefficients of the Taylor expansion at small k are functions of these two master integrals. Using these expansions, we could check that the various two-point functions behave as expected.

Let us also mention that the regularity of $\Gamma^\parallel(k)$ in the limit $k \to 0$ can alternatively be seen as a consequence of the Slavnov-Taylor identity (18) and the fact that $\Gamma(k)$ vanishes at least as k^2, or, equivalently, the fact that $\Gamma(k)$ vanishes at least as k^2 can be seen as a consequence of the Slavnov-Taylor identity and the regularity of $\Gamma^\parallel(k)$.

4. Spurious singularities

The limit $k \to 0$ is not the only one where individual terms in the reduced expression for $\Gamma^C(k)$ behave in a singular manner. In the case of the ghost and gluon two-point functions, we find that certain terms are singular as k^2 approaches $2m^2$ or $2M^2$. Of course, the two-point function in these limits should be regular, thus providing a test for the reduced expressions. We have checked that this is indeed the case since the residue of $1/(k^2 - 2x^2)$ with $x = m$ or $x = M$ vanishes thanks to the following identity between master integrals ($k_x \equiv \sqrt{2}x$)

$$2(d-3)x^2\left[6(d-4)x^4 M_{xxxx0}(k_x^2) - (3d-8)S_{xx0}(k_x^2)\right]$$
$$= \left[(d-2)A_x - 2(d-3)x^2 B_{xx}(k_x^2)\right]^2 - 8(d-3)^2 x^4 B_{xx}^2(k_x^2), \quad (58)$$

that one can derive using the Laporta algorithm. When expanded in ϵ, it is easily shown that this combination is finite and reproduces the combination of finite master integrals in Eq. (23) of Ref. [37] that was also found to vanish using the results in Ref. [58].

In addition, all two-point functions contain terms that are singular as m approaches $2M$. Since the Euclidean two-point functions have no reason to be singular in this limit, some cancellations need to occur among these terms, providing a further check on the reduced expressions. For instance, in the case of $\Gamma^1(k)$, we found a potentially singular term at $m = 2M$, the residue of $1/(m - 2M)$ being proportional to

$$(d-2)(2A_M - A_{2M})B_{M(2M)}(k)$$
$$+ 4M^2\Big(T_{M(2M)(2M)}(k) - 2T_{(2M)(2M)M}(k)$$
$$- (d-3)U_{(2M)M(2M)M}(k)\Big). \quad (59)$$

Using the Laporta algorithm, we verified that this combination of master integrals indeed vanishes. In particular we built a different REDUZE database to the two mass scale one described earlier. Instead a single mass scale database was constructed where we set $m_a = M$ and $m_b = 2M$ at the outset. These cancellations played a role in other two-point functions. In the case of the gluon two-point function, we needed several other vanishing combinations of master integrals. These are

$$(d-2)(2A_M - A_{2M})B_{MM}(k)$$
$$- 4M^2\Big(T_{M(2M)M}(k)$$
$$- 2T_{(2M)MM}(k)$$
$$- (d-3)U_{MM(2M)M}(k)\Big), \quad (60)$$

$$(d-2)A_M B_{(2M)(2M)}$$
$$+ 2M^2\Big(T_{M(2M)M} + (d-3)U_{(2M)(2M)MM}\Big), (61)$$

and finally

$$(d-3)\left[(d-4)k^2 x^2(k^2+4x^2)^2 M_{xxxx0} - 2(3d-8)(k^2+4x^2)S_{xx0}\right]$$
$$= \left[(d-2)^2 A_x^2 - 2(d-2)(d-3)k^2 A_x B_{xx} - 2(d-3)^2 k^2 x^2 B_{xx}^2\right](k^2+4x^2)$$
$$- 4(d-3)\left[3p^2 T_{xx0} + 4(d-3)(k^2+x^2)U_{0(2x)xx} - 2(d-2)(k^2+x^2)A_x B_{(2x)x}\right](k^2-2x^2) \quad (62)$$

that we also substantiated using the Laporta algorithm. This later cancellation boils down to (58) when $k^2 = 2x^2$.

5. Zero mass limit

This is more an internal cross-check since we computed independently the propagators in the case of vanishing gluon and quark mass ($M = m = 0$) with the goal of recovering them from the zero mass limit of the massive propagators. In order to compute this limit it is useful to bare in mind that any of the master integrals presented above can be written as

$$(\mu^{2\epsilon})^L \mathcal{F}(k^2, m^2, M^2) = (\mu^{2\epsilon})^L (k^2)^D$$
$$\times \mathcal{F}(1, m^2/k^2, M^2/k^2), \quad (63)$$

where L is the number of loops and D the mass dimension of the integral (leaving aside the powers of μ that

multiply it). As a result of this simple dimensional analysis it is clear that the low mass expansion ($m \ll k$ and $M \ll k$ simultaneously) is equivalent to the large momentum expansion. Consequently, the zero quark and gluon mass limits for $\Gamma(k)$, $\Gamma^\perp(k)$, $\Gamma^\gamma(k)$ are nothing but the leading terms in the expansions (49)-(51). We have checked that these expressions coincide with the results of a direct calculation with massless fields (in the minimal subtraction scheme). Of course, in this limit, $\Gamma^\parallel(k)$ and $\Gamma^1(k)$ are just zero.

IV. RENORMALIZATION GROUP

In principle, in order to compare the renormalized two-point functions computed within a given approach to those obtained within lattice simulations, it is enough to evaluate the renormalized two-point functions at a given renormalization scale, that is $\Gamma^C(k; \mu_0)$. Indeed, the momentum dependence of renormalized two-point functions as computed within different approaches should differ only to within an overall constant which is easily adjusted.

In practice, however, a direct perturbative evaluation of $\Gamma^C(k; \mu_0)$, such as the one described in the previous section, is not accurate in the case of a large separation of scales between k and μ_0. Indeed, in this case, large logarithms $\ln k/\mu_0$ effectively modify the expansion parameter λ into $\lambda \ln k/\mu_0$ which has no reason to be small, even when λ is small. As is well known, the way to cope with these large logarithms is to use the renormalization group (RG).

The renormalized functions $\Gamma^C(k; \mu)$ for different values of μ are related by the fact that they arise from the same bare function $\Gamma^C(k)$. The differential equation governing the evolution of $\Gamma^C(k; \mu)$ with μ is the so-called Callan-Szymanzik equation. In its integrated form it can be written as

$$
\begin{aligned}
&\Gamma^C(k; m_0^2, M_0, \lambda_0, \mu_0) \\
&= z_C^{-1}(\mu, \mu_0)\, \Gamma^C(k; m^2(\mu), M(\mu), \lambda(\mu), \mu)
\end{aligned} \quad (64)
$$

and relates a given n-point function at the fixed scale μ_0 to the same n-point function at the running scale μ. The benefit of Eq. (64) is that it allows one to evaluate $\Gamma^C(k; \mu_0)$ while maintaining perturbative control at any scale. This is achieved by evaluating the right-hand side of Eq. (64) with the choice $\mu = k$ that prevents the appearance of any large logarithms. This requires in turn the evaluation of the rescaling factor $z_C(\mu, \mu_0)$ as well as the running $m^2(\mu)$, $M(\mu)$ and $\lambda(\mu)$ of the various parameters.

The rescaling factor is given by

$$
z_C(\mu, \mu_0) = \exp\left(\int_{\mu_0}^{\mu} d\nu\, \gamma_C(\nu)\right), \quad (65)
$$

where γ_C is the so-called anomalous dimension related to

the corresponding renormalization factor Z_C as

$$
\gamma_C \equiv \frac{d\ln Z_C}{d\ln \mu}. \quad (66)
$$

The running of the parameters is given by the so-called beta functions

$$
\beta_{m^2} \equiv \frac{dm^2}{d\ln \mu}, \quad \beta_M \equiv \frac{dM}{d\ln \mu}, \quad \beta_{g^2} \equiv \frac{dg^2}{d\ln \mu}. \quad (67)
$$

It should be noted that the derivatives $d/d\ln \mu$ in Eqs. (66)-(67) are to be taken for fixed bare masses and dimensionful bare coupling $\Lambda^{2\epsilon} Z_{g^2} g^2$. These constraints imply[6]

$$
0 = \gamma_{m^2} + \frac{\beta_{m^2}}{m^2} = \gamma_M + \frac{\beta_M}{M} = \gamma_{g^2} + \frac{\beta_{g^2}}{g^2}, \quad (68)
$$

where

$$
\gamma_{m^2} \equiv \frac{d\ln Z_{m^2}}{d\ln \mu}, \quad \gamma_M \equiv \frac{d\ln Z_M}{d\ln \mu} \text{ and } \gamma_{g^2} \equiv \frac{d\ln Z_{g^2}}{d\ln \mu} \quad (69)
$$

are the anomalous dimension associated with the parameters.

Thus, in a sense, the renormalization group allows us to evaluate $\Gamma^C(k; \mu_0)$ by using perturbation theory indirectly: rather than using perturbation theory to evaluate $\Gamma^C(k; \mu_0)$, one uses perturbation theory to determine all the anomalous dimensions

$$
\gamma_X \equiv \frac{d\ln Z_X}{d\ln \mu}, \quad (70)
$$

(with $X \in \{C, m^2, M, g^2\}$) from which one can reconstruct the running of the parameters and the rescaling factors that enter (64). As we discuss in App. B, the anomalous dimensions do not have large logarithms and are thus amenable to perturbative calculations.[7] In the next section, we explain how the two-loop anomalous dimensions are evaluated.

A. Two-loop anomalous dimensions and beta functions in the IR-safe scheme

In a generic renormalization scheme, the renormalization conditions allow us to access the various renormalization factors Z_X with $X \in \{A, c, \psi, m^2, M, \lambda\}$ from which one can evaluate the corresponding anomalous dimensions γ_X. More precisely, from

$$
Z_X = 1 + \lambda \frac{z_{X,1}}{\epsilon} + \lambda^2 \frac{z_{X,2}}{\epsilon}, \quad (71)
$$

---

[6] These equations are easily obtained by requiring that the logarithms of $Z_{m^2} m^2$, $Z_M M$ and $\Lambda^{2\epsilon} Z_{g^2} g^2$ do not depend on $\ln \mu$. Here we are taking a μ-independent Λ. In App. B, we discuss the case of a μ-dependent Λ, including the conventional choice of $\Lambda = \mu$.

[7] This true, of course, provided $\lambda(\mu)$ remains moderate enough.

with $z_{X,1} = z_{X,11} + z_{X,10}\epsilon + z_{X,1(-1)}$ and $z_{X,2} = z_{X,22} + z_{X,21}\epsilon + z_{X,20}\epsilon^2$ where the $z_{X,ab}$ are functions of Λ, μ, m^2 and M, it is possible to derive the following generic expression for the anomalous dimension:

$$\gamma_X = g^2 \frac{\partial z_{X,10}}{\partial \ln \mu} + g^4 \left(\frac{\partial z_{X,20}}{\partial \ln \mu} - \left(\frac{\partial z_{X,10}}{\partial \ln \mu} + \frac{\partial z_{g^2,10}}{\partial \ln \mu} \right) z_{X,10} - \left(\frac{\partial z_{X,1(-1)}}{\partial \ln \mu} + \frac{\partial z_{g^2,1(-1)}}{\partial \ln \mu} \right) z_{X,11} - \sum_i \frac{\partial z_{m_i^2,10}}{\partial \ln \mu} \frac{\partial z_{X,10}}{\partial \ln m_i^2} \right), \tag{72}$$

where $\sum_i$ sums over all possible masses in the problem, here $m_i = m$ and $m_i = M$. See App. B for details. Moreover, the finiteness of the anomalous dimensions requires the following constraints to hold true

$$0 = \frac{\partial z_{X,11}}{\partial \ln \mu} = \frac{\partial z_{X,22}}{\partial \ln \mu}$$
$$= \frac{\partial}{\partial \ln \mu} \Big(z_{X,21} - (z_{X,10} + z_{g^2,10}) z_{X,11} \Big). \tag{73}$$

The first two are trivial since, as we have already seen $z_{X,11}$ and $z_{X,22}$ are pure constants. The last constraint is less trivial and we have checked that it holds true in the particular renormalization scheme considered here. It should of course hold true in any other renormalization scheme. In particular, we show in App. C that this constraint is nothing but a generalization of the constraint $z_{X,22} = z_{X,11}(z_{X,11} + z_{g^2,11})/2$ that arises as a consequence of the finiteness of the anomalous dimensions within the minimal subtraction renormalization scheme.

We mention also that, in the case where $z_{X,11} \neq 0$, the above constraints can be used to simplify the formula (72) by rewriting the second term within the round bracket by $-\frac{z_{X,10}}{z_{X,11}} \frac{\partial z_{X,21}}{\partial \ln \mu}$. When $z_{X,11} = 0$, this replacement cannot be made but the formula simplifies as well because the third term within the bracket vanishes. In the present model, this occurs for the quark anomalous dimension since $z_{\psi,11} = 0$.

As we have already mentioned above, in this work we consider the so-called IR-safe renormalization scheme defined by the conditions (19)-(21). In addition to the benefits of this choice which were already reviewed in Sec. II C, we note that the use of (19) allows us to bypass the calculation of the anomalous dimensions for m^2 and λ since they are directly given in terms of the anomalous dimensions for A and c via

$$\gamma_\lambda = -(\gamma_A + 2\gamma_c), \quad \gamma_{m^2} = -(\gamma_A + \gamma_c), \tag{74}$$

leading to the beta functions

$$\frac{\beta_\lambda}{\lambda} = \gamma_A + 2\gamma_c, \quad \frac{\beta_{m^2}}{m^2} = \gamma_A + \gamma_c. \tag{75}$$

Moreover, one can formally solve this system for γ_A and γ_c in terms of linear combinations of β_{m^2}/m^2 and β_λ/λ

giving

$$\gamma_A = \frac{\beta_\lambda}{\lambda} - 2\frac{\beta_{m^2}}{m^2}, \quad \gamma_c = \frac{\beta_{m^2}}{m^2} - \frac{\beta_\lambda}{\lambda}. \tag{76}$$

Then, one can explicitly integrate the rescaling factors $z_A(\mu, \mu_0)$ and $z_c(\mu, \mu_0)$ in terms of the running parameters $m^2(\mu)$ and $\lambda(\mu)$

$$z_A(\mu, \mu_0) = \frac{m_0^4}{\lambda_0} \frac{\lambda(\mu)}{m^4(\mu)}, \quad z_c(\mu, \mu_0) = \frac{\lambda_0}{m_0^2} \frac{m^2(\mu)}{\lambda(\mu)}. \tag{77}$$

This, combined with the renormalization conditions (20), provides explicit expressions for the gluon and ghost dressing functions in terms of the running parameters

$$D(p; \mu_0) = \frac{\lambda_0}{m_0^4} \frac{m^4(p)}{\lambda(p)} \frac{p^2}{p^2 + m^2(p)}, \tag{78}$$

$$F(p; \mu_0) = \frac{m_0^2}{\lambda_0} \frac{\lambda(p)}{m^2(p)}. \tag{79}$$

For the quark propagator, we need to determine the quark mass anomalous dimension in order to extract the corresponding beta function, as well as the quark anomalous dimension in order to obtain the corresponding rescaling factor. However, with the parametrization (15), the rescaling factor applies only to $Z(k)$, and because of the renormalization condition, we have

$$Z(k; \mu_0) = \exp\left(-\int_{\mu_0}^k d\nu \, \gamma_\psi(\nu) \right). \tag{80}$$

As already mentioned, the quark mass function $M(k)$ identifies with the running mass in the chosen scheme.

B. Asymptotic behaviors

In Apps. D and E, the interested reader can find the UV and IR asymptotic expansion of the various two-loop anomalous dimensions at next-to-leading order, which we used in order to control the RG flow in these regimes.

With the RG flow at our disposal, we can now evaluate the various two-point functions and compare to available lattice data.

V. RESULTS

In this section, we compare the unquenched ghost, gluon and quark dressing functions as well as the quark mass function, as computed within the CF model at two-loop order, to existing SU(3) four dimensional lattice data in the case of two degenerate quark flavors. Our results depend on three parameters defined at the initial scale μ_0 of the RG flow: the renormalized coupling $\lambda_0 = \lambda(\mu_0)$, the renormalized gluon mass $m_0 = m(\mu_0)$ and the renormalized quark mass $M_0 = M(\mu_0)$. In addition to these three parameters, we have adjustable normalization factors $\mathcal{N}_X$ for $X \in \{F, D, Z\}$. There is not such an adjustable normalization for the quark mass function since the latter is a scheme independent quantity.

In order to find the best fit to the lattice data, the parameters and the normalizations need to be chosen so as to minimize a joint error function χ combining the individual errors χ_X, with $X \in \{F, D, Z, M\}$:

$$\chi^2 \equiv \frac{1}{4}\left[\chi_F^2 + \chi_D^2 + \chi_Z^2 + \chi_M^2\right]. \tag{81}$$

The individual error for $X \in \{F, D, Z\}$ is taken to be

$$\chi_X^2 = \frac{1}{N}\sum_i \left(\mathcal{N}_X \frac{X_{\text{th.}}(k_i)}{X_{\text{lt.}}(k_i)} - 1\right)^2, \tag{82}$$

which simply averages, over the available data points, the relative error of the appropriately rescaled theoretical values $X_{\text{th.}}(k_i)$ to the data $X_{\text{lt.}}(k_i)$. This choice is justified because the data for $X \in \{F, D, Z\}$ never become small over the available range; see below. In contrast, when $X = M$, the data decrease rapidly as one increases k and it makes more sense to consider an average of relative errors, in the range where the data are not small, and of appropriately normalized absolute errors, in the range where the data become small. In this case, we shall then employ the error function

$$\chi_M^2 = \frac{1}{N}\left[\sum_{i=1}^{i=*}\left(\frac{M_{\text{th.}}(k_i)}{M_{\text{lt.}}(k_i)} - 1\right)^2 \right.$$
$$\left. + \sum_{i=*+1}^{i=N}\left(\frac{M_{\text{th.}}(k_i)}{M_{\text{lt.}}(k_*)} - \frac{M_{\text{lt.}}(k_i)}{M_{\text{lt.}}(k_*)}\right)^2\right], \tag{83}$$

where k_* is chosen such that $M_{\text{lt.}}(k_*)$ is the point from the lattice data closest to 0.1 GeV.

Because the error function (81) depends quadratically on the normalizations $\mathcal{N}_X$, the latter can be determined explicitly in terms of the lattice and theoretical data. One finds

$$\mathcal{N}_X = \frac{\sum_i X_{\text{th.}}(k_i)/X_{\text{lt.}}(k_i)}{\sum_i X_{\text{th.}}^2(k_i)/X_{\text{lt.}}^2(k_i)}. \tag{84}$$

The fitting problem reduces then to the minimization of χ^2 with respect to the three remaining parameters, λ_0, m_0 and M_0.

A. Far from the chiral limit

We first compare our two-loop results with lattice data simulated using a pion mass $M_\pi = 426$ MeV, see Refs. [52, 74], that is relatively far from the chiral limit. The set of parameters that minimizes χ and the corresponding errors are shown in Tab. I. The corresponding plots for the gluon and ghost dressing functions are shown in Fig. 4, whereas those for the quark mass function and quark dressing function are shown in Fig. 5. It is also instructive to display the individual errors as obtained from this global fit. This is shown in Tab. II.
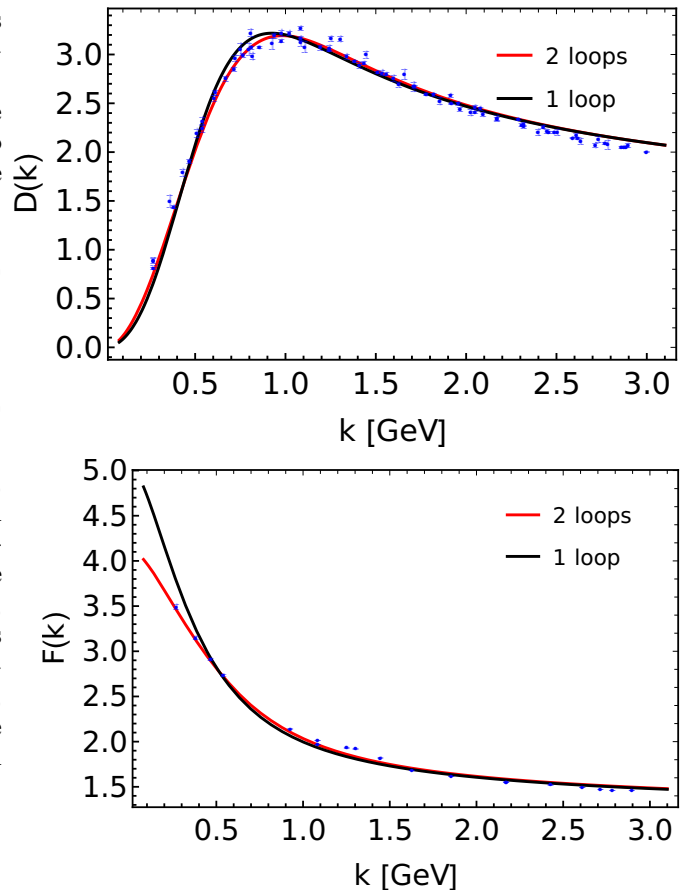

FIG. 4. Comparison of the one- and two-loop CF results for the gluon (top) and ghost (bottom) dressing functions to the lattice data of Ref. [52] using $M_\pi = 426$ MeV. The parameters are determined from a global fit using the four functions D, F, Z and M and the lattice data of Refs. [52, 74].

order	λ_0	m_0	M_0	$\chi(\%)$
1-loop	0.39	430	140	13.0
2-loop	0.32	390	160	5.6

TABLE I. Parameters that minimize χ comparing with lattice data for $M_\pi = 426$ MeV. The parameters m_0 and M_0 are given in MeV and μ_0 is taken equal to 1 GeV.
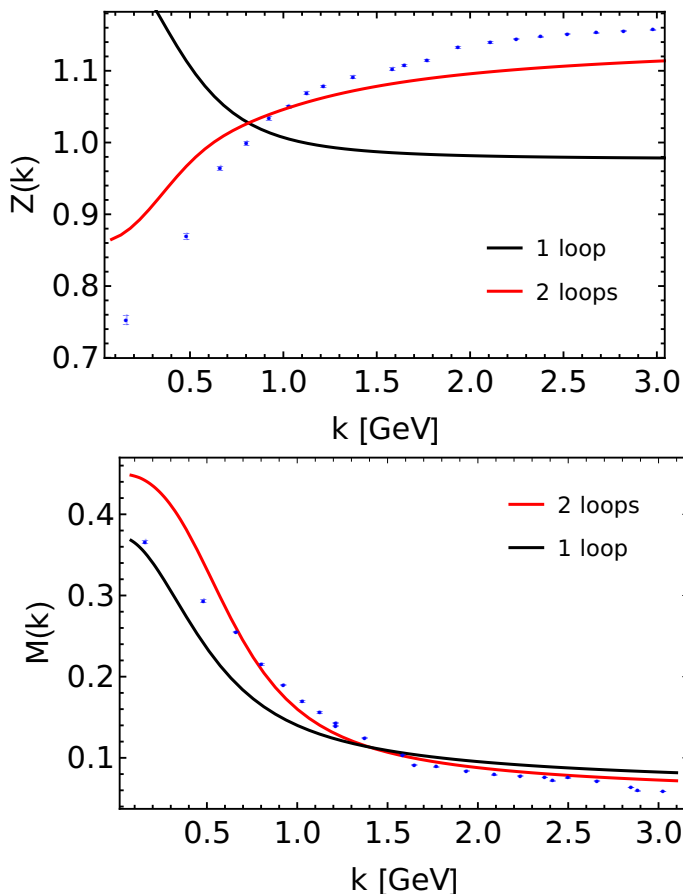
FIG. 5. Comparison of the one- and two-loop CF results for the quark dressing function (top) and quark mass function (bottom) to the lattice data of Ref. [74] using $M_\pi = 426$ MeV. The parameters are determined from a global fit using the four functions D, F, Z and M and the lattice data of Refs. [52, 74].

order	$\chi_F(\%)$	$\chi_D(\%)$	$\chi_Z(\%)$	$\chi_M(\%)$
1-loop	3.3	5.3	19.3	16.1
2-loop	2.4	3.7	5.3	9.0

TABLE II. Individual errors as obtained from the global fit of Tab. I.

We observe that the global agreement with lattice data greatly improves once two-loop corrections are included. Moreover, two-loop contributions appear to be small in the ghost-gluon sector, as expected [42]. This suggests that perturbation theory is well controlled in the gauge sector of the CF model. On the other hand, the improvement on the quark dressing function is quite remarkable, given the inconsistent results obtained at one-loop for this quantity [1]. As already mentioned earlier, this is an indication that the quark dressing function is well described by perturbation theory within the CF model, the mismatch of the one-loop results just meaning that one needs to go at least up to two-loop order to start having a good account of the function. In fact the error χ_Z is

comparable to χ_F and χ_D, the plot in Fig. 5 being here a little bit misleading since it zooms in on a region close to $Z = 1$.[8] This confirms earlier expectations based on estimates of the two-loop corrections [1].

The largest source of error comes clearly from the quark mass function although we note that the error values obtained for χ_M remain quite reasonable and still improve when including the two-loop corrections. As already mentioned above, this can be attributed to the fact that the lattice data are relatively far from the chiral limit and non-perturbative considerations are not needed to generate the corresponding quark mass. In fact, if we exclude the quark mass function from the fit (by using the error function $\tilde{\chi}$ defined below in (85)), the corresponding errors for F, D and Z at two-loop order remain essentially the same, with a clear improvement of Z, see Tab. III.

order	$\chi_F(\%)$	$\chi_D(\%)$	$\chi_Z(\%)$
1-loop	5.5	3.9	16.1
2-loop	2.5	3.7	3.0

TABLE III. Individual errors as obtained from a fit that excludes the function M.

We expect of course the ability of perturbation theory to reproduce the quark mass function to decrease as we try to fit lattice data closer to the chiral limit. We investigate this question in the next section.

B. Closer to the chiral limit

The deterioration of the quality of perturbation theory with regard to the quark mass function is related to the fact that perturbation theory is not capable of capturing the spontaneous breaking of chiral symmetry. As already discussed in Sec. II D, within the CF model, this can be consistently cured by employing a double expansion in powers of the pure gauge coupling and of the inverse number of colors. We shall not consider this strategy here, however, since our aim is to remain at a purely perturbative level. Instead, we shall investigate to which extent the dressing functions D, F and Z remain under perturbative control despite the increasing tension in the quark mass function as we approach the chiral limit. To this purpose, we consider global fits that include or exclude the quark mass function and which are thus based

---

[8] In a certain sense, the leading order perturbative contribution to the quark dressing function is the two-loop contribution. Based on this remark, it would be even more consistent to fit the lattice propagators using the two-loop expressions for F, D and M and the three-loop expressions for Z. A complete three-loop evaluation of Z is a difficult task but one could imagine doing a rough estimate similar to the estimate made in Ref. [1] for the two-loop corrections.

either on the error function (81) or on the reduced error function

$$\tilde{\chi}^2 = \frac{1}{3}\left[\chi_F^2 + \chi_D^2 + \chi_Z^2\right]. \tag{85}$$

In this latter case, we can consider the parameter M_0 either as a free parameter that needs to be varied along with the other parameters λ_0 and m_0, or fix it such that the quark mass function agrees with the lattice data at some momentum scale in the UV. For this analysis, we shall use the most chiral data available to date [52, 74] that correspond to a pion mass of $M_\pi = 150$ MeV.
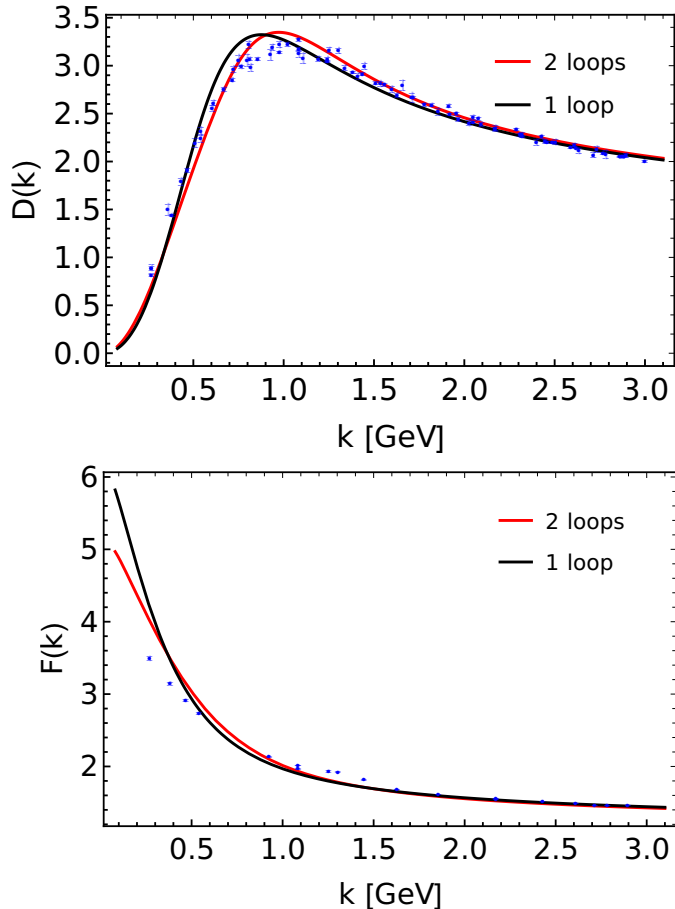

FIG. 6. Comparison of the one- and two-loop CF results for the gluon (top) and ghost (bottom) dressing functions to the lattice data of Ref. [52] using $M_\pi = 150$ MeV. The parameters are determined from a global fit using the four functions D, F, Z and M and the lattice data of Refs. [52, 74].

The parameters of the global fit including all functions are given in Tab. IV together with the global error. The individual errors are displayed in Tab. V. The corresponding plots are shown in Figs. 6 and 7.

As expected, the perturbative description of the quark mass function deteriorates, although we note that there is still an improvement when including the two-loop corrections and the two-loop result captures a substantial part of the quark mass function for the
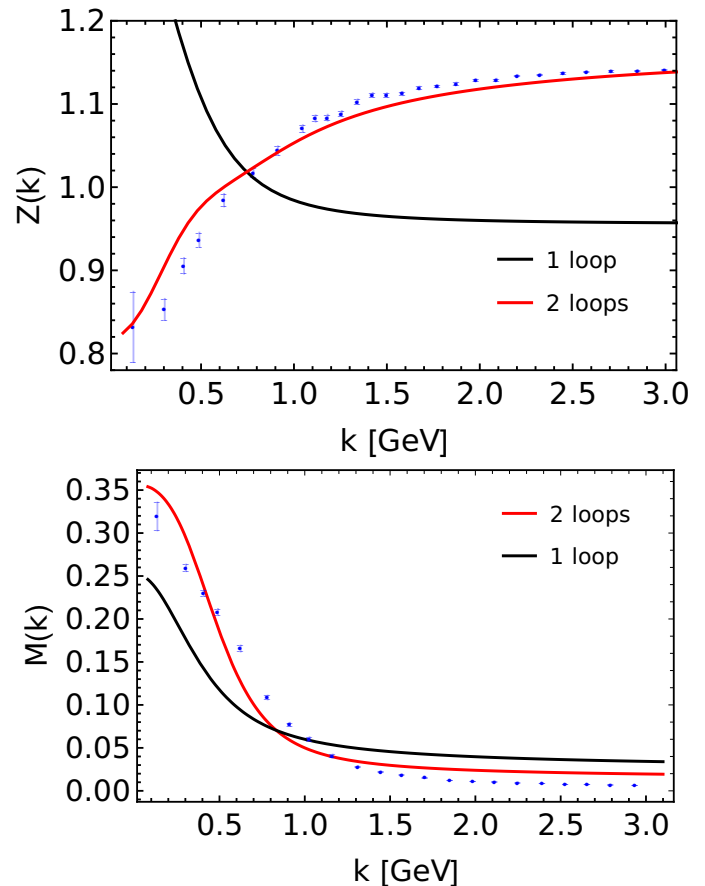

FIG. 7. Comparison of the one- and two-loop CF results for the quark dressing function (top) and quark mass function (bottom) to the lattice data of Ref. [74] using $M_\pi = 150$ MeV. The parameters are determined from a global fit using the four functions D, F, Z and M and the lattice data of Refs. [52, 74].

order	λ_0	m_0	M_0	$\chi(\%)$
1-loop	0.41	400	60	17.6
2-loop	0.36	360	50	7.5

TABLE IV. Parameters that minimize χ comparing with lattice data for $M_\pi = 150$ MeV. The parameters m_0 and M_0 are given in MeV and μ_0 is taken equal to 1 GeV.

considered value of M_π, specially in the infrared. This deterioration in the fit of the quark mass slightly impacts the errors on the other functions (specially the ghost and quark dressing functions in the infrared) which remain, however, well described by the perturbative expressions.

When excluding the quark mass function from the global fit, a clear improvement on the ghost, gluon and even quark dressing functions is visible both on the plots given in Figs. 8 and on the error values, see Tab. VI. This confirms that these quantities are well described by perturbation theory within the CF model, even for close

order	$\chi_F(\%)$	$\chi_D(\%)$	$\chi_Z(\%)$	$\chi_M(\%)$
1-loop	6.3	6.1	20.6	27.3
2-loop	5.6	5.1	1.9	12.7

TABLE V. Individual errors as obtained from the global fit of Tab. IV.

to physical values of the pion mass. In fact, the errors are surprisingly smaller than in the case of $M_\pi = 426$ MeV, see Tab. III. The parameters which minimize the reduced joint error (85) remain similar to the ones computed before, and the joint error is less sensitive to the value of M_0 value than it is to the values of the other parameters, as can be seen in Fig. 9. We note finally that the quality of the fits at $M_\pi = 150$ MeV seems to be even better than that obtained for $M_\pi = 426$ MeV. A closer look reveals that, when the mass is included in the fit, the improvement only truly occurs for the function Z, the other functions F, D and M presenting larger errors than in the case $M_\pi = 426$ MeV. The curve for M does quite well in reproducing the IR data, but presents an offset in the UV tail which impacts our estimation of the error. As the mass function is excluded from the fit, the quality of the fit for Z remains quite good (and even improves further) and the errors on the functions F and D become comparable to those obtained for $M_\pi = 426$ MeV. This confirms that the only quantity that cannot be accessed within a strict perturbative approach within the CF model is the mass function M, in the case where the quarks are too light, although we stress once more that the IR is quite well reproduced, even for physical quark masses, if one allows for a small offset in the UV.

order	$\chi_F(\%)$	$\chi_D(\%)$	$\chi_Z(\%)$
1-loop	4.9	4.0	14.3
2-loop	2.4	3.3	1.3

TABLE VI. Individual errors as obtained from a global fit that excludes the quark mass function, to be compared to the individual errors as given in Tab. V.

Rather than considering M_0 as a free parameter, one can also adjust it such that the quark mass function agrees with the lattice data at some momentum in the UV, i.e. 2.94 GeV, corresponding to a quark mass of 6.6 MeV. Since in the present scheme, the quark mass function and the renormalized mass agree with each other, this adjustment is easily achieved by choosing the initial condition of the RG flow at $\mu_0 = 2.94$ GeV, with $M_0 = 6.6$ MeV, leaving only two parameters, λ_0 and m_0, to minimize $\tilde{\chi}$.

Enforcing the quark mass in the UV to the lattice value introduces of course some tension that deteriorates (mainly in the infrared) the quality of our results for the various dressing functions (not shown). However, our
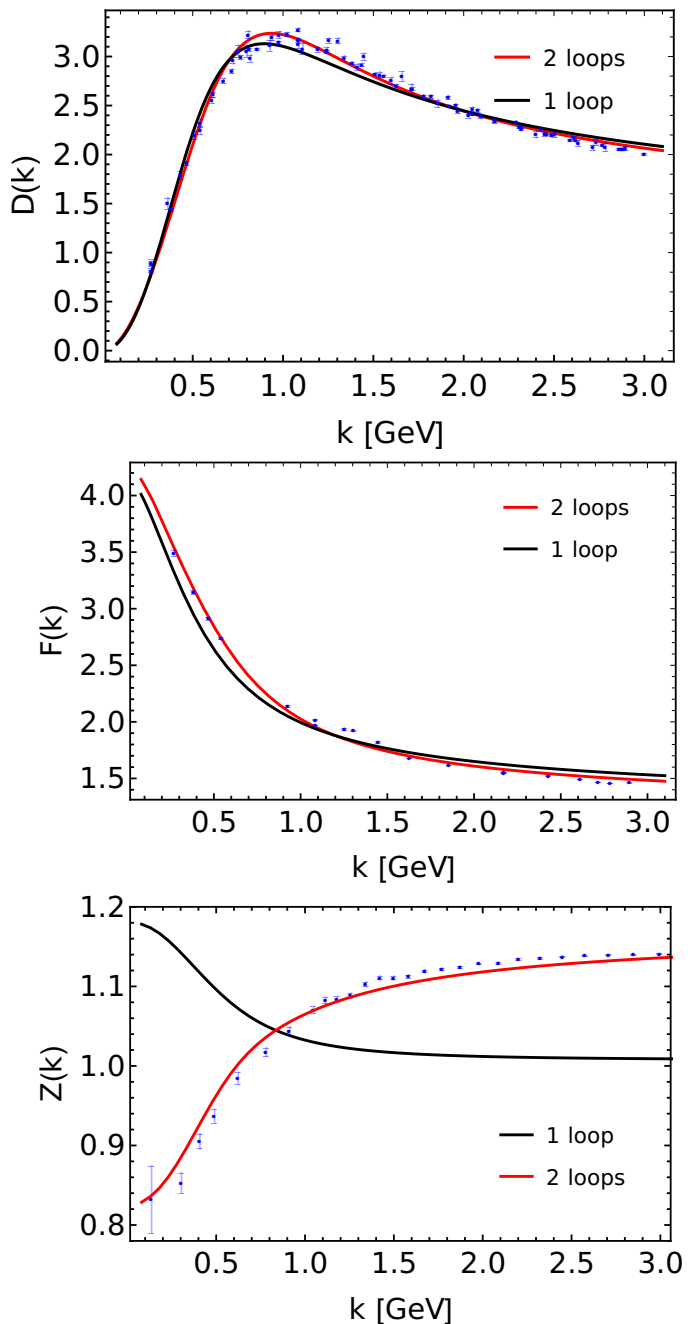

FIG. 8. Comparison of the one- and two-loop CF results for the gluon (top) and ghost (middle) and quark (bottom) dressing functions to the lattice data of Ref. [52] using $M_\pi = 150$ MeV. The parameters are determined from a global fit using the three functions D, F, Z and the lattice data of Refs. [52, 74].

purpose here is to evaluate the role of two-loop perturbative corrections in generating the quark mass function in the infrared for a small (but non-zero) value of M_π. Our result for the quark mass function is shown in Fig. 10. We find that, for $M_\pi = 150$ MeV, the constituent quark mass is only reproduced to 10% accuracy at one-loop
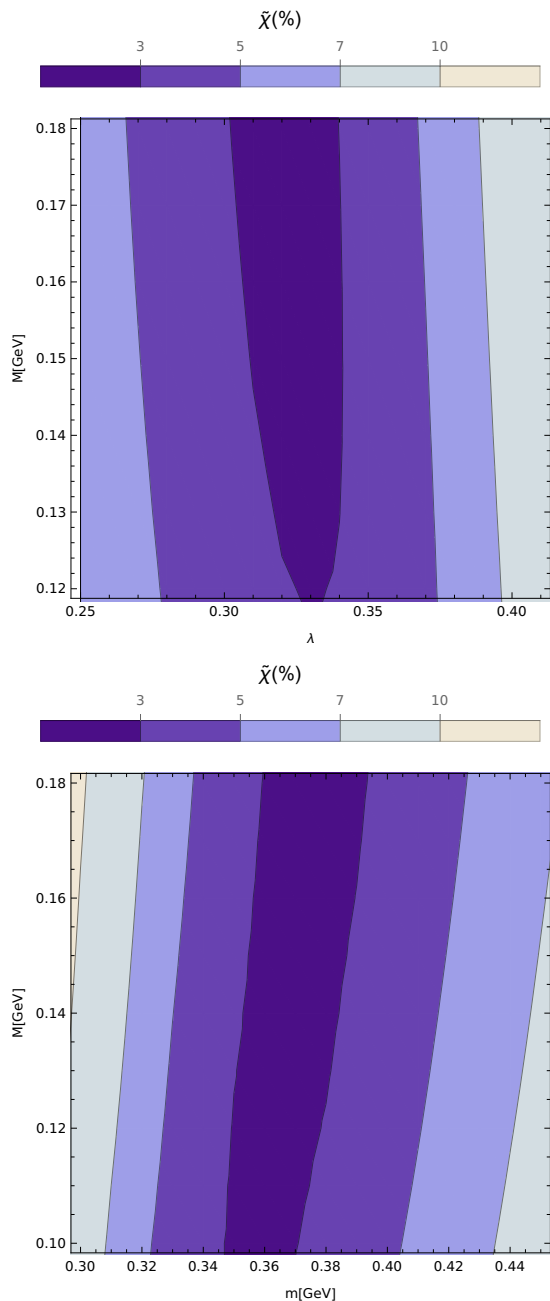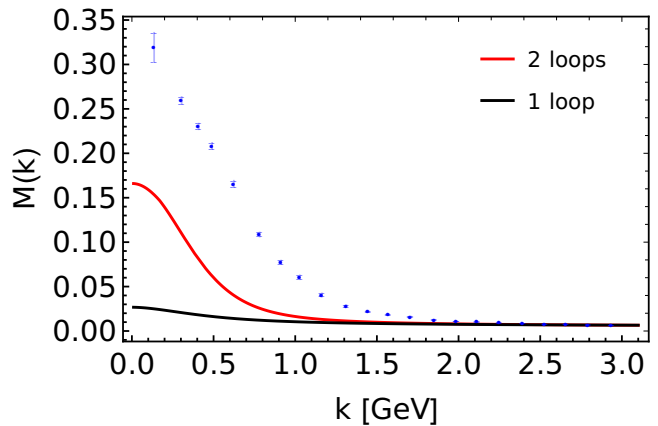
FIG. 10. Comparison of the one- and two-loop CF results for the quark mass function to the lattice data of Ref. [74] using $M_\pi = 150$ MeV. The parameters λ_0 and m_0 are determined from a global fit using the four functions D, F, Z and the lattice data of Refs. [52, 74]. The parameter M_0 is chosen to coincide with the lattice data at the scale $\mu_0 = 2.94$ GeV.

C. A remark on the used data for Z

We have used two kinds of lattice data for the quark dressing function Z, as described in Ref. [74]. In the first set, the same lattice action is used to describe the whole range of momenta, while in the second set an improved action has been used for momenta larger than ~ 2 GeV in the case $M_\pi = 426$ MeV, and larger than ~ 1 GeV in the case $M_\pi = 150$ MeV. While we used the improved data to produce the plots shown above, strangely enough, our fits for Z are systematically better when using the non-improved data set. We note, however, that the differences are rather small and can probably not be resolved at the present level of accuracy.

VI. CONCLUSIONS

In this work, we have performed an exhaustive investigation of all two-point correlation functions of the Curci-Ferrari model in the presence of degenerate fundamental quark flavors, using the IR-safe renormalization scheme that was put forward in Ref. [25]. We were able to evaluate all the two-loop graphs using a variety of techniques. Moreover we were able to construct smooth plots of the form factors over all energies that incorporated the running of all parameters. This was necessary to compare with specific lattice data sets which depended on different choices of the pion mass.

By comparing our results to available lattice data for QCD two-point functions in the case of two degenerate flavors, we find that the ghost and gluon dressing functions are well captured by the perturbative expansion within the CF model both far from the chiral limit and closer to the physical case. This was already known from

FIG. 9. Level curves for the reduced error function $\tilde{\chi}$ in parameter space. The top plot shows the error regions for a fixed value of the gluon mass, $m_0 = 380$ MeV, while for the bottom plot we fixed the coupling in such a way that $\lambda_0 = 0.32$.

order while we can obtain 50% of its value by including two-loop contributions. As already mentioned above, the full dressing function can be generated using the RI expansion but it is already interesting to note that two-loop perturbative corrections are conspiring in the right direction.

one-loop evaluations within this model [1] and two-loop corrections represent tiny corrections to these already accurate results.

The impact of two-loop corrections by contrast is more important in the quark sector where they drastically correct for the qualitatively inconsistent quark dressing function obtained at one-loop order. Our conclusion is that the two-loop contribution represents the true leading order contribution to the quark dressing function and provides as accurate results as for the other dressing functions.

As for the quark mass function, it is well known that in principle it cannot be described within a strict perturbative approach, especially close to the chiral limit. We find, however, that even in the case of an almost physical value for the pion mass, the two-loop corrections provide a non-negligible part of the quark mass function and that the mismatch has little impact on the accuracy of the various dressing functions.

In a future work, we plan to extend the analysis to the quark-gluon vertex in those particular configurations where one of the external momenta vanishes, similar to the analysis of the ghost-antighost-gluon vertex given in Ref. [39]. The challenge is here again to reduce all the Feynman integrals that enter the various form factors. However, since one of the external momenta vanishes, this is of the same complexity as the evaluation of the two-point form factors. Moreover, no additional renormalization group analysis needs to be carried out since all the relevant beta functions and anomalous dimensions have been evaluated in the present work.

Appendix A: Diagrams

1. Gluon two-point function

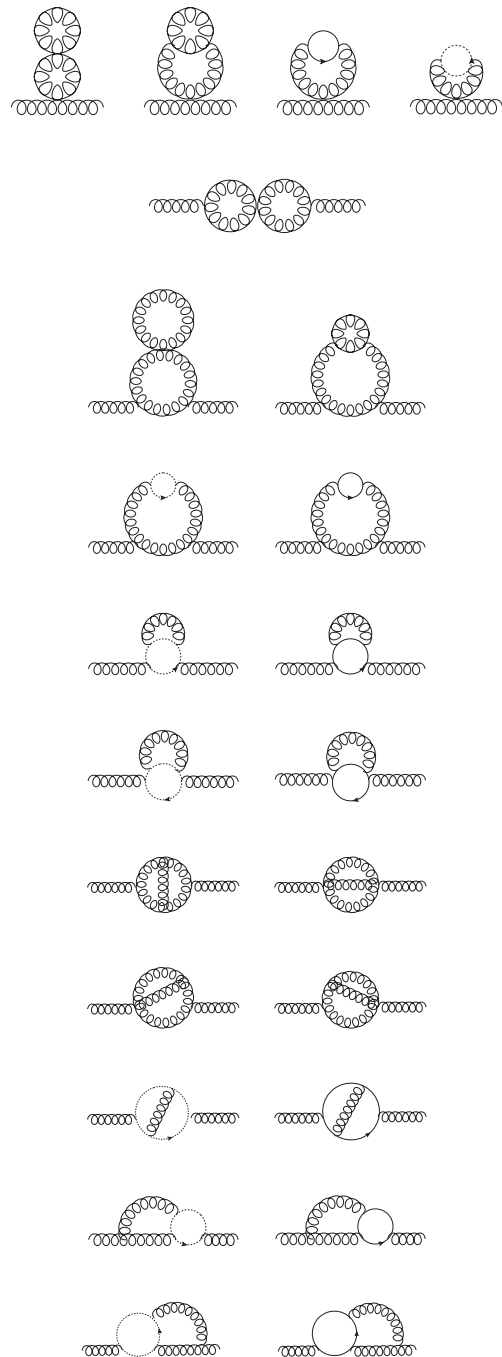The two-loop diagrams contributing to the gluon two-point function are displayed in Fig. 11.

FIG. 11. Two-loop diagrams contributing to the gluon two-point function.

2. Ghost two-point function

The two-loop diagrams contributing to the ghost two-point function are displayed in Fig. 12.
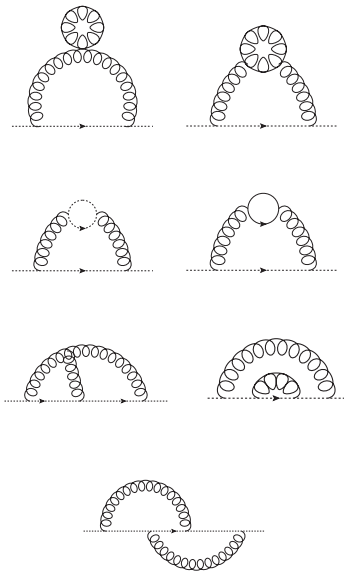

FIG. 12. Two-loop diagrams contributing to the ghost two-point function.

3. Quark two-point function

The two-loop diagrams contributing to the quark two-point function are displayed in Fig. 13.
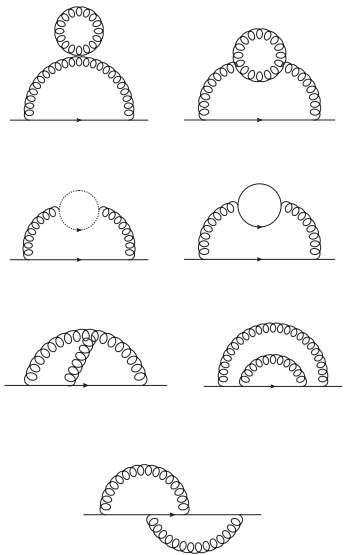

FIG. 13. Two-loop diagrams contributing to the quark two-point function.

Appendix B: Two-loop running

In this section, we derive general formulas for the two-loop anomalous dimensions and beta functions within a generic renormalization scheme defined from a given set of renormalization conditions, such as for instance the IR-safe conditions considered in this work. In Sec. C, for completeness, we shall also revisit the minimal subtraction scheme and see how it fits the general discussion (despite the absence of renormalization conditions in this case).

We consider a field theory involving various bare fields $\varphi_{B,i}$ of bare square mass $m_{B,i}^2$. For simplicity, we assume that interactions are controlled by only one bare coupling, denoted by λ_B, but an extension to an arbitrary number of coupling constants is straightforward. We work in dimensional regularization, in which case the bare coupling has dimension $4 - d = 2\epsilon$ and it is convenient to make this explicit by introducing a scale. We shall then operate the rescaling $\lambda_B \to \Lambda^{2\epsilon}\lambda_B$ where the new λ_B is dimensionless. As already mentioned in the main text, our notational choice Λ (rather than μ) is not innocent. It is meant to emphasize that this scale is in general different from the renormalization scale μ. The latter is introduced upon implementing a certain renormalization scheme via the renormalization conditions. On the other hand, the scale Λ is a regulating scale that has nothing to do with the renormalization procedure.

To some extent, the scale Λ should be put on the same footing as the cut-off scale in the cut-off regularization. This analogy needs to be taken with a pinch of salt of course because, in dimensional regularization, the regulating parameter ϵ is dissociated from the regulating scale Λ. In particular, the continuum limit is defined as the limit $\epsilon \to 0$ and not as the limit $\Lambda \to \infty$. However, as in any other regularization, we expect the continuum results obtained in the limit $\epsilon \to 0$, to be independent of the regulating scale Λ, while they will in general depend on the renormalization scale μ. This should apply in particular to the anomalous dimensions and the beta functions and we will check explicitly that this is indeed the case.

Let us mention that, in most approaches, the scale Λ is identified with the scale μ. This is a perfectly acceptable choice (and even a convenient one in some respects)[9] since the anomalous dimensions and the beta functions do not depend on this choice and are in fact the same for any choice of dependence $\Lambda(\mu)$. However, the choice of a μ-dependent Λ tends to obscure the real source of μ-dependence within the renormalization group, while unnecessarily complicating the evaluation of the anomalous dimensions and the beta functions (as we shall explicitly

—————

[9] In particular, one does not need to introduce two scales in intermediate calculations. We stress however that continuum results do not depend on the scale Λ, so they depend only on one scale, μ, even in the case where the choice $\Lambda \neq \mu$ is made.

illustrate below). In what follows, we shall first derive the anomalous dimensions and the beta functions by taking Λ independent from μ and then check that the so obtained functions do not depend on the choice of Λ, even when the latter is assumed to depend on μ.

1. RG basics

Upon renormalization, the bare fields and the bare parameters are rescaled by renormalization factors as

$$\varphi_{B,i} = Z_{\varphi_i}^{1/2}\varphi_i, \ \ m_{B,i}^2 = Z_{m_i^2}m_i^2, \ \ \lambda_B = Z_\lambda\lambda. \quad \text{(B1)}$$

We shall denote the renormalization factors generically as Z_X with $X \in \{\varphi_i, m_i^2, \lambda\}$. They depend a priori on the regulator ϵ, the two scales Λ and μ, and the renormalized parameters m_i^2 and g^2.

The renormalized n-point functions are functions of the renormalization scale μ. This μ-dependence is controlled by the Callan-Szymanzik equation which, in its integrated form, is written as[10]

$$\Gamma^{(n)}_{\varphi_{i_1}\dots\varphi_{i_n}}(\{k\}; \{m_0^2\}, \lambda_0, \mu_0) \quad \text{(B2)}$$
$$= \prod_{k=1}^n z_{i_k}^{-1/2}(\mu, \mu_0)\, \Gamma^{(n)}_{\varphi_{i_1}\dots\varphi_{i_n}}(\{k\}; \{m^2(\mu)\}, \lambda(\mu), \mu),$$

and relates a given n-point function at a fixed scale μ_0 to the same n-point function at the running scale μ. We have already discussed the benefit of this type of equations in maintaining perturbative when large logarithms are present. Perturbative control is achieved by evaluating the right-hand side of Eq. (B2) with the choice $\mu = k$. This requires in turn the evaluation of the rescaling factor $z(\mu, \mu_0)$ as well as the running $m_i^2(\mu)$ and $\lambda(\mu)$ of the various parameters.

The rescaling factor is given by

$$z_i(\mu, \mu_0) = \exp\left(\int_{\mu_0}^\mu d\nu\, \gamma_{\varphi_i}(\nu)\right), \quad \text{(B3)}$$

where γ_{φ_i} is the so-called anomalous dimension of the field φ_i, related to the corresponding renormalization factor Z_{φ_i} as

$$\gamma_{\varphi_i} \equiv \frac{d\ln Z_{\varphi_i}}{d\ln\mu}, \quad \text{(B4)}$$

where the $d/d\ln\mu$ derivatives are to be taken for fixed bare masses and dimensionful bare coupling $\Lambda^{2\epsilon}Z_\lambda\lambda$. On the other hand, the running of the parameters is given by the so-called beta functions

$$\beta_\lambda \equiv \frac{d\lambda}{d\ln\mu}, \quad \beta_{m_i^2} \equiv \frac{dm_i^2}{d\ln\mu}. \quad \text{(B5)}$$

By expressing that $\ln(Z_{m_i^2}m_i^2)$ and $\ln(\Lambda^{2\epsilon}Z_\lambda\lambda)$ do not depend on $\ln\mu$, one easily relates the beta functions to the anomalous dimensions associated with the parameters as[11]

$$0 = \gamma_{m_i^2} + \frac{\beta_{m_i^2}}{m_i^2}, \quad 0 = \gamma_\lambda + \frac{\beta_\lambda}{\lambda}, \quad \text{(B6)}$$

where

$$\gamma_{m_i^2} \equiv \frac{d\ln Z_{m_i^2}}{d\ln\mu} \quad \text{and} \quad \gamma_\lambda \equiv \frac{d\ln Z_\lambda}{d\ln\mu} \quad \text{(B7)}$$

It follows that the implementation of the renormalization group equation (B2), requires the determination of the various anomalous dimensions

$$\gamma_X \equiv \frac{d\ln Z_X}{d\ln\mu}, \quad \text{(B8)}$$

with $X \in \{\varphi_i, m_i^2, \lambda\}$. Below, we evaluate these anomalous dimensions at one- and two-loop order.

We mention that, in deriving Eq. (B6), we have made use of our assumption of a μ-independent Λ. Were we to consider a μ-dependent Λ, the right-hand side of the second equation of (B6) would involve an additional term $2\epsilon\, d\ln\Lambda/d\ln\mu$ which cannot be neglected because it can (and does) end up multiplying contributions proportional to $1/\epsilon$. By choosing a μ-independent Λ, we do not need to worry about this subtlety. A related convenient feature of using a μ-independent Λ is that both $\beta_{m_i^2}/m_i^2$ and β_λ/λ are of order λ, whereas with a μ-dependent Λ, β_λ/λ is of order λ^0 which leads to new contributions when evaluating the anomalous dimensions at a given order. We will show below that despite these implementation differences, the various additional contributions that one needs to consider in the case of a μ-dependent Λ cancel with each other, making the μ-independent choice, the simpler one in practice.

We also stress that the success of the perturbative RG relies on the absence of large logarithms in the right-hand side of Eq. (B2) which is granted by the choice $\mu = k$ but also by the fact that the anomalous dimensions do not contain large logarithms. This last property is rather intuitive since anomalous dimensions are usually associated with variations of the system over a thin momentum shell. However, it is satisfactory to see explicitly why large logarithms are absent from the anomalous dimensions. We shall provide an answer to this question below. Needless to mention that the anomalous dimensions are finite functions for they enter the RG evolution of renormalized n-point functions. This property will be put into good use below.

---

[10] We use the notation $\{k\}$ and $\{m^2\}$ to designate respectively the set of all external momenta of the considered n-point function and the set of all masses in the problem.

[11] For the moment, we take Λ as μ-independent. We later discuss the case of a μ-dependent Λ, including the conventional choice $\Lambda = \mu$.

2. One-loop running

To derive the anomalous dimension γ_X at one-loop order, we start from the one-loop renormalization factor Z_X expanded up to order ϵ^0. We write it as

$$Z_X = 1 + \lambda \frac{z_{X,1}}{\epsilon} \,, \tag{B9}$$

with

$$z_{X,1} = z_{X,11} + \epsilon z_{X,10} \,, \tag{B10}$$

and where $z_{X,11}$ and $z_{X,10}$ are a priori functions of Λ, μ and the masses m_i^2. We will see below that there are some constraints on the factors $z_{X,ab}$.

From (B8) and (B9), the anomalous dimension becomes

$$\gamma_X = \frac{1}{Z_X} \left(\frac{\lambda}{\epsilon} \frac{\partial z_{X,1}}{\partial \ln \mu} + \frac{\beta_\lambda}{\lambda} \frac{\lambda}{\epsilon} z_{X,1} \right.$$
$$\left. + \sum_i \frac{\beta_{m_i^2}}{m_i^2} \frac{\lambda}{\epsilon} \frac{\partial z_{X,1}}{\partial \ln m_i^2} \right). \tag{B11}$$

The term with the partial derivative $\partial/\partial\mu$ takes into account the explicit μ-dependence of $z_{X,1}$, while the terms involving the beta functions, see Eq. (B5), take into account the implicit μ-dependence of $z_{X,1}$ via its dependence on λ and m_i^2. Since $\beta_{m_i^2}/m_i^2$ and β_λ/λ are of order λ, see the discussion above, we can neglect the terms proportional to the beta functions to the present order of accuracy. Moreover, we can replace Z_X by 1 in the denominator of (B11). We find eventually

$$\gamma_X = \frac{\lambda}{\epsilon} \frac{\partial z_{X,1}}{\partial \ln \mu} \,. \tag{B12}$$

Expanding to order ϵ^0, this gives

$$\gamma_X = \frac{\lambda}{\epsilon} \frac{\partial z_{X,11}}{\partial \ln \mu} + \lambda \frac{\partial z_{X,10}}{\partial \ln \mu} \,. \tag{B13}$$

The finiteness of the anomalous dimensions imposes $z_{X,11}$ not to depend explicitly on μ. This is not really a surprise since $z_{X,11}/\epsilon$ corresponds to the divergence of a one-loop Feynman integral and, as such, is a pure constant that does not depend on the considered renormalization scheme. We eventually arrive at

$$\gamma_X = \lambda \frac{\partial z_{X,10}}{\partial \ln \mu} \,. \tag{B14}$$

We notice that the anomalous dimension could a priori still depend on Λ (via the factor $z_{X,10}$). We will show below that this is not the case and also that the same expression could be obtained using a μ-dependent Λ.

3. Two-loop running

In order to extend the anomalous dimension γ_X to two-loop order, we need the renormalization factors to order λ^2 and ϵ^1, which we write as

$$Z_X = 1 + \lambda \frac{z_{X,1}}{\epsilon} + \lambda^2 \frac{z_{X,2}}{\epsilon^2} \,, \tag{B15}$$

with

$$z_{X,1} = z_{X,11} + z_{X,10}\epsilon + z_{X,1(-1)}\epsilon^2 \,, \tag{B16}$$
$$z_{X,2} = z_{X,22} + z_{X,21}\epsilon + z_{X,20}\epsilon^2 \,. \tag{B17}$$

We need to include $z_{X,1(-1)}$ because, although it is a contribution of order ϵ^1 to Z_X, it contributes at order ϵ^0 to the two-loop two-point functions; see the discussion in the main text. We will see below that it also contributes to the anomalous dimensions at this order.

From (B8) and (B15), the anomalous dimension becomes

$$\gamma_X = \frac{1}{Z_X} \left(\frac{\lambda}{\epsilon} \frac{\partial z_{X,1}}{\partial \ln \mu} + \frac{\lambda^2}{\epsilon^2} \frac{\partial z_{X,2}}{\partial \ln \mu} + \frac{\beta_\lambda}{\lambda} \left(\lambda \frac{z_{X,1}}{\epsilon} + 2\lambda^2 \frac{z_{X,2}}{\epsilon^2} \right) + \sum_i \frac{\beta_{m_i^2}}{m_i^2} \left(\frac{\lambda}{\epsilon} \frac{\partial z_{X,1}}{\partial \ln m_i^2} + \frac{\lambda^2}{\epsilon^2} \frac{\partial z_{X,2}}{\partial \ln m_i^2} \right) \right). \tag{B18}$$

Using the fact that $\beta_{m_i^2}/m_i^2$ and β_λ/λ are both of order λ and expanding Z_X up to order λ, we find

$$\gamma_X = \frac{\lambda}{\epsilon} \frac{\partial z_{X,1}}{\partial \ln \mu} + \frac{\lambda^2}{\epsilon^2} \frac{\partial z_{X,2}}{\partial \ln \mu} - \frac{\lambda^2}{\epsilon^2} \frac{\partial z_{X,1}}{\partial \ln \mu} z_{X,1} - \gamma_\lambda \frac{\lambda}{\epsilon} z_{X,1} - \sum_i \gamma_{m_i^2} \frac{\lambda}{\epsilon} \frac{\partial z_{X,1}}{\partial \ln m_i^2} \,, \tag{B19}$$

where γ_λ and γ_{m^2} are the gamma functions determined at one-loop order, prior to an expansion in ϵ, see Eq. (B12). Using this latter equation, we find

$$\gamma_X = \frac{\lambda}{\epsilon} \frac{\partial z_{X,1}}{\partial \ln \mu} + \frac{\lambda^2}{\epsilon^2} \left(\frac{\partial z_{X,2}}{\partial \ln \mu} - \left(\frac{\partial z_{X,1}}{\partial \ln \mu} + \frac{\partial z_{\lambda,1}}{\partial \ln \mu} \right) z_{X,1} - \sum_i \frac{\partial z_{m_i^2,1}}{\partial \ln \mu} \frac{\partial z_{X,1}}{\partial \ln m_i^2} \right), \tag{B20}$$

and expanding to order ϵ^0, this gives

$$\gamma_X = \frac{\lambda^2}{\epsilon^2}\frac{\partial z_{X,22}}{\partial \ln \mu} + \frac{\lambda^2}{\epsilon}\left(\frac{\partial z_{X,21}}{\partial \ln \mu} - \left(\frac{\partial z_{X,10}}{\partial \ln \mu} + \frac{\partial z_{\lambda,10}}{\partial \ln \mu}\right)z_{X,11}\right) + \lambda\frac{\partial z_{X,10}}{\partial \ln \mu}$$
$$+ \lambda^2\left(\frac{\partial z_{X,20}}{\partial \ln \mu} - \left(\frac{\partial z_{X,10}}{\partial \ln \mu} + \frac{\partial z_{\lambda,10}}{\partial \ln \mu}\right)z_{X,10} - \left(\frac{\partial z_{X,1(-1)}}{\partial \ln \mu} + \frac{\partial z_{\lambda,1(-1)}}{\partial \ln \mu}\right)z_{X,11} - \sum_i \frac{\partial z_{m_i^2,10}}{\partial \ln \mu}\frac{\partial z_{X,10}}{\partial \ln m_i^2}\right), \quad \text{(B21)}$$

where we used that $z_{X,11}$ is a pure constant. The finiteness of the gamma function imposes that

$$\frac{\partial z_{X,22}}{\partial \ln \mu} = 0 \quad \text{and} \quad \frac{\partial z_{X,21}}{\partial \ln \mu} - \left(\frac{\partial z_{X,10}}{\partial \ln \mu} + \frac{\partial z_{\lambda,10}}{\partial \ln \mu}\right)z_{X,11} = 0. \quad \text{(B22)}$$

The first constraint is again not a real surprise since $z_{X,22}/\epsilon^2$ has to do with the overall divergence of a two-loop Feynman integral and, as such, should be a pure constant that does not depend on the considered renormalization scheme. The second constraint is more subtle and relates to a similar well known identity in minimal subtraction which constrains $z_{X,22}$, $z_{X,11}$, $z_{\lambda,11}$, see below. Since $z_{X,11}$ is a pure constant, this second constraint can also be reformulated as stating that the combination $z_{X,21} - (z_{X,10} + z_{\lambda,10})z_{X,11}$ should not depend on μ. In turn, this provides a cross-check for any two-loop determination of the n-point functions in a given scheme, which we have used in our particular application to the CF model. See the main text.

We eventually arrive at the following finite expression for the two-loop anomalous dimension

$$\gamma_X = \lambda\frac{\partial z_{X,10}}{\partial \ln \mu} + \lambda^2\left(\frac{\partial z_{X,20}}{\partial \ln \mu} - \left(\frac{\partial z_{X,10}}{\partial \ln \mu} + \frac{\partial z_{\lambda,10}}{\partial \ln \mu}\right)z_{X,10} - \left(\frac{\partial z_{X,1(-1)}}{\partial \ln \mu} + \frac{\partial z_{\lambda,1(-1)}}{\partial \ln \mu}\right)z_{X,11} - \sum_i \frac{\partial z_{m_i^2,10}}{\partial \ln \mu}\frac{\partial z_{X,10}}{\partial \ln m_i^2}\right),$$
$$\text{(B23)}$$

in terms of the various factors $z_{X,ab}$. In the case $z_{X,11} \neq 0$, this expression can be simplified using the second constraint in (B22). One finds

$$\gamma_X = \lambda\frac{\partial z_{X,10}}{\partial \ln \mu} + \lambda^2\left(\frac{\partial z_{X,20}}{\partial \ln \mu} - \frac{z_{X,10}}{z_{X,11}}\frac{\partial z_{X,21}}{\partial \ln \mu} - \left(\frac{\partial z_{X,1(-1)}}{\partial \ln \mu} + \frac{\partial z_{\lambda,1(-1)}}{\partial \ln \mu}\right)z_{X,11} - \sum_i \frac{\partial z_{m_i^2,10}}{\partial \ln \mu}\frac{\partial z_{X,10}}{\partial \ln m_i^2}\right). \quad \text{(B24)}$$

In the case $z_{X,11} = 0$, one cannot use the second constraint but the formula also gets simpler:

$$\gamma_X = \lambda\frac{\partial z_{X,10}}{\partial \ln \mu} + \lambda^2\left(\frac{\partial z_{X,20}}{\partial \ln \mu} - \left(\frac{\partial z_{X,10}}{\partial \ln \mu} + \frac{\partial z_{\lambda,10}}{\partial \ln \mu}\right)z_{X,10} - \sum_i \frac{\partial z_{m_i^2,10}}{\partial \ln \mu}\frac{\partial z_{X,10}}{\partial \ln m_i^2}\right). \quad \text{(B25)}$$

In the case $z_{X,11} \neq 0$, we note that the anomalous dimensions involve $z_{X,1(-1)}$ and $z_{\lambda,1(-1)}$, that is order ϵ^1 contributions to the renormalization factors. This, in turn, can be traced back to the fact that the one-loop anomalous dimensions that appear in Eq. (B19) are multiplied by $1/\epsilon$ and, therefore, need to be expanded up to order ϵ^1, contrary to the previous section where they were expanded up to order ϵ^0 only. That the terms with $z_{X,1(-1)}$ and $z_{\lambda,1(-1)}$ are not present in the case $z_{X,11} = 0$ is also visible in Eq. (B19) since the just mentioned $1/\epsilon$ terms are not present.

4. Λ-independence

The formula (B23) and its simplified versions (B24) and (B25) are the ones we use in our implementation of the RG in Sec. IV. We still need to clarify two questions however.

First, the expression (B23) was derived assuming a μ-independent Λ and one is left wondering what would happen with a μ-dependent Λ (such as the standard choice $\Lambda = \mu$). We will show that one obtains exactly the same expressions for the anomalous dimension γ_X, via a lengthier procedure however. Second, even though the expression (B23) does not depend explicitly on Λ, it could still depend implicitly on Λ via the dependence of the factors $z_{X,ab}$. We will show that this is not so: the Λ-dependence cancels identically when the various $z_{X,ab}$ are combined into Eq. (B23).

A key remark in demystifying these two questions is that the only source of Λ-dependence in the renormalization factors appears via the ϵ-expansion of $\Lambda^{2\epsilon}\lambda$ (since the scale Λ is introduced as a rescaling of the coupling in the first place). In practice this means that, if the renormalization factors are written as

$$Z_X = 1 + \sum_{a \geq 1}\left(\frac{\lambda}{\epsilon}\right)^a z_{X,a}, \quad \text{(B26)}$$

one should have $\partial(\Lambda^{-2a\epsilon} z_{X,a})/\partial \ln \Lambda = 0$, that is

$$\frac{\partial z_{X,a}}{\partial \ln \Lambda} - 2a\epsilon z_{X,a} = 0 \,. \qquad (B27)$$

Writing each $z_{X,a}$ as

$$z_{X,a} = \sum_{b \leq a} z_{X,ab} \, \epsilon^{a-b} \,, \qquad (B28)$$

the constraint (B27) can be rewritten as

$$\frac{\partial z_{X,ab}}{\partial \ln \Lambda} = 2a z_{X,a(b+1)} \,, \qquad (B29)$$

for $b < a$, and

$$\frac{\partial z_{X,aa}}{\partial \ln \Lambda} = 0 \,, \qquad (B30)$$

this later result being totally trivial since the $z_{X,aa}$ are expected to be pure constants, independent of the considered renormalization scheme.

a. Explicit Λ-dependence

Keeping these remarks in mind, let us now re-derive the one-loop anomalous dimensions using a μ-dependent Λ. There are two main differences with respect to the calculation that used a μ-independent Λ. First, there is a new source of μ-dependence in the renormalization factors, via Λ. This leads to the expression

$$\gamma_X = \frac{1}{Z_X} \left(\frac{\lambda}{\epsilon} \frac{\partial z_{X,1}}{\partial \ln \mu} + \frac{\lambda}{\epsilon} \frac{\partial z_{X,1}}{\partial \ln \Lambda} \frac{d \ln \Lambda}{d \ln \mu} \right.$$
$$\left. + \frac{\beta_\lambda}{\lambda} \frac{\lambda}{\epsilon} z_{X,1} + \sum_i \frac{\beta_{m_i^2}}{m_i^2} \frac{\lambda}{\epsilon} \frac{\partial z_{X,1}}{\partial \ln m_i^2} \right), \quad (B31)$$

where we note the presence of a new term proportional to $d \ln \Lambda / d \ln \mu$ as compared to (B11). Second, there is an additional term in the relation between the beta function and the anomalous dimension for λ, see (B6):

$$0 = 2\epsilon \frac{d \ln \Lambda}{d \ln \mu} + \gamma_\lambda + \frac{\beta_\lambda}{\lambda} \,. \qquad (B32)$$

When expanding the anomalous dimension (B31) up to order λ, this term cannot be neglected unlike γ_λ because 1) it is of one order less in λ as compared to γ_λ and therefore produces a new order λ contribution, and 2) this new contribution survives the continuum limit since it has the form $\epsilon \times 1/\epsilon$. One eventually arrives at

$$\gamma_X = \frac{\lambda}{\epsilon} \frac{\partial z_{X,1}}{\partial \ln \mu} + \lambda \left(\frac{1}{\epsilon} \frac{\partial z_{X,1}}{\partial \ln \Lambda} - 2z_{X,1} \right) \frac{d \ln \Lambda}{d \ln \mu} \,. \quad (B33)$$

A similar but lengthier calculation at two-loop order leads to (B19) supplemented with the term

$$\left[\left(\lambda - \frac{\lambda^2}{\epsilon} z_{X,1} \right) \left(\frac{1}{\epsilon} \frac{\partial z_{X,1}}{\partial \ln \Lambda} - 2z_{X,1} \right) \right.$$
$$\left. + \frac{\lambda^2}{\epsilon} \left(\frac{1}{\epsilon} \frac{\partial z_{X,2}}{\partial \ln \Lambda} - 4z_{X,2} \right) \right] \frac{d \ln \Lambda}{d \ln \mu} \,. \quad (B34)$$

Owing to Eq. (B27), it is easy to see that all these extra terms that one generates when evaluating the anomalous dimension with a μ-dependent Λ eventually cancel. As announced above, the final expression for the anomalous dimension in terms of the factors $z_{X,a}$ does not depend on the particular choice of Λ, and the fastest way to arrive at the result (avoiding unnecessary cancellations) is to use a μ-independent Λ.

b. Implicit Λ-dependence

So far we have shown that the expressions (B12) and (B19) have no explicit dependence on Λ. Obviously, this conclusion extends to (B14) and (B23) which are nothing but the order ϵ^0 truncated versions of these expressions. However, there could still be an implicit dependence with respect to Λ via the factors $z_{X,ab}$. We now show that this is not the case.

Consider for instance (B14) and take a $\partial/\partial \ln \Lambda$ derivative. Owing to Eq. (B29), we have

$$\frac{\partial \gamma_X}{\partial \ln \Lambda} = \lambda \frac{\partial^2 z_{X,10}}{\partial \ln \mu \partial \ln \Lambda} = 2\lambda \frac{\partial z_{X,11}}{\partial \ln \mu} \,, \qquad (B35)$$

which vanishes since $z_{X,11}$ is a pure constant.

A similar conclusion can be reached starting from the two-loop expression (B23) and exploiting (B29). Focusing on the terms inside the bracket multiplying λ^2, we find

$$\frac{\partial}{\partial \ln \Lambda} \left(\dots \right)_{\lambda^2} = 4 \frac{\partial z_{X,21}}{\partial \ln \mu} - 2 \left(\frac{\partial z_{X,11}}{\partial \ln \mu} + \frac{\partial z_{\lambda,11}}{\partial \ln \mu} \right) z_{X,10} - 2 \left(\frac{\partial z_{X,10}}{\partial \ln \mu} + \frac{\partial z_{\lambda,10}}{\partial \ln \mu} \right) z_{X,11}$$
$$- 2 \left(\frac{\partial z_{X,10}}{\partial \ln \mu} + \frac{\partial z_{\lambda,10}}{\partial \ln \mu} \right) z_{X,11} - \left(\frac{\partial z_{X,1(-1)}}{\partial \ln \mu} + \frac{\partial z_{\lambda,1(-1)}}{\partial \ln \mu} \right) \frac{\partial z_{X,11}}{\partial \ln \Lambda}$$
$$- 2 \sum_i \frac{\partial z_{m_i^2,11}}{\partial \ln \mu} \frac{\partial z_{X,10}}{\partial \ln m_i^2} - 2 \sum_i \frac{\partial z_{m_i^2,10}}{\partial \ln \mu} \frac{\partial z_{X,11}}{\partial \ln m_i^2} = 4 \left(\frac{\partial z_{X,21}}{\partial \ln \mu} - \left(\frac{\partial z_{X,10}}{\partial \ln \mu} + \frac{\partial z_{\lambda,10}}{\partial \ln \mu} \right) z_{X,11} \right) = 0 \,,$$
$$(B36)$$

where we have again used that $z_{X,11}$ is a pure constant, as well as the second constraint in (B22).

We mention that, contrary to the absence of explicit Λ-dependence, the absence of implicit Λ-dependence applies only to the anomalous dimensions in the continuum limit $\epsilon \to 0$. For instance, the one-loop anomalous dimension to order ϵ^1

$$\gamma_X = \lambda \frac{\partial z_{X,10}}{\partial \ln \mu} + \lambda \frac{\partial z_{X,1(-1)}}{\partial \ln \mu} \,, \qquad \text{(B37)}$$

depends implicitly on Λ since one has

$$\frac{\partial \gamma_X}{\partial \ln \Lambda} = \lambda \frac{\partial^2 z_{X,1(-1)}}{\partial \ln \mu \partial \ln \Lambda} = 2\lambda \frac{\partial z_{X,10}}{\partial \ln \mu} \,, \qquad \text{(B38)}$$

which is usually not zero. As we already discussed above, this Λ-dependent, order ϵ^1 one-loop anomalous dimension is crucial for the correct evaluation of the order ϵ^0 two-loop anomalous dimension since it is multiplied by a $1/\epsilon$ factor in Eq. (B19). In this case, however, the Λ-dependence (B38) gets cancelled by other Λ-dependent terms in the ϵ^0 order two-loop anomalous dimension, thus ensuring the Λ-independence of the latter.

5. Absence of large logarithms in γ_X

The previous considerations allow us to understand more precisely the absence of large logarithms in the anomalous dimensions, which we alluded to above. Indeed, the renormalization factors are functions of Λ/m_i and μ/m_i and large logarithms could potentially occur when any of these ratios goes to 0 or ∞. However, if we assume that the renormalization scheme is regular in the $m_i \to 0$ limit (this is the case for the IR-safe scheme considered in this work), the renormalization factors need to have a well defined zero-mass limit and therefore large logarithms associated with $\Lambda/m_i \to \infty$ or $\mu/m_i \to \infty$ are excluded. We are then left with potential large logarithms in the limits $\Lambda/m_i \to 0$ or $\mu/m_i \to 0$. However, there cannot be large logarithms associated with $\mu/m_i \to 0$ because $m_i \gg \mu$ and the Feynman integrals that enter the renormalization factors are always infrared regulated.[12] In conclusion, the only possible source of large logarithms in the renormalization factors is $\Lambda/m_i \to 0$. But because the anomalous dimensions do not depend on Λ, these large logarithms in the renormalization factors are not inherited by the anomalous dimensions. We stress that the previous argument excludes the presence only of large logarithms in the anomalous dimensions and beta functions. Of course, the latter can feature logarithms multiplied by strictly positive (resp.

strictly negative) powers of m^2/μ^2 in the UV (resp. in the IR), as the explicit expressions given in App. **??** illustrate.

6. Non-renormalization theorems

The formula for the two-loop anomalous dimensions that we have derived above is general. It may happen, as in the model considered in this work, that some of the renormalization factors obey a non-renormalization theorem stating that their product $\prod_i Z_{X_i}$ is finite and allowing one to consider a scheme where this product is set equal to 1. This, in turn, implies the relation $\sum_i \gamma_{X_i} = 0$ between the corresponding anomalous dimensions.

Let us here check that the general formula (B20) is compatible with this expectation. The non-renormalization theorem implies

$$0 = \sum_i z_{X_i,1} \,, \qquad \text{(B39)}$$

$$0 = 2\sum_i z_{X_i,2} + \sum_{i \neq j} z_{X_i,1} z_{X_j,1} \,. \qquad \text{(B40)}$$

Owing to (B39), it is trivial to check that the terms of (B20) that are linear in $z_{X,1}$ cancel in the sum $\sum_i \gamma_{X_i}$. To check that the remaining terms cancel as well, we use (B39) in order to rewrite (B40) as

$$0 = 2\sum_i z_{X_i,2} - \sum_i z_{X_i,1}^2 \,. \qquad \text{(B41)}$$

Then, the remaining terms in (B20) are proportional to

$$\sum_i \left(\frac{\partial z_{X_i,2}}{\partial \ln \mu} - \frac{\partial z_{X_i,1}}{\partial \ln \mu} z_{X_i,1} \right)$$

$$= \frac{1}{2} \frac{\partial}{\partial \ln \mu} \sum_i (2z_{X_i,2} - z_{X_i,1}^2) = 0 \,. \qquad \text{(B42)}$$

Appendix C: Minimal subtraction

Up until now, we have restricted our attention to renormalization schemes associated with renormalization conditions. In this section, for completeness, we revisit the minimal subtraction scheme which relies, not on renormalization conditions, but rather on the strict absorption of $1/\epsilon$ poles in the renormalization factors. We will show that, despite appearances, this scheme fits the general discussion of the previous section.

In the minimal subtraction scheme, renormalization factors contain purely divergent terms in the limit $\epsilon \to 0$ (whose pre-factors are pure constants), and do not involve any finite part. At two-loop order for instance, we

---

[12] This does not prevent the appearance of terms like $\mu^2/m^2 \ln \mu^2/m^2$ but these are not large logarithms for $\mu/m \to 0$.

have

$$Z_X = 1 + \lambda \frac{z_{X,1}^{\overline{MS}}}{\epsilon} + \lambda^2 \frac{z_{X,2}^{\overline{MS}}}{\epsilon^2}, \qquad \text{(C1)}$$

with $z_{X,1}^{\overline{MS}} = z_{X,11}$ and $z_{X,2}^{\overline{MS}} = z_{X,22} + \epsilon z_{21}^{\overline{MS}}$,[13] and thus $z_{X,10}^{\overline{MS}} = z_{X,1(-1)}^{\overline{MS}} = z_{X,20}^{\overline{MS}} = 0$. Naïvely, it seems that one cannot use the formulas (B14) and (B23) for these would give simply 0. Moreover, it seems that there is no point in distinguishing between a renormalization scale μ and a regulating scale Λ as we did above since there are no renormalization conditions to introduce the renormalization scale μ in the first place.

On the other hand, the only scale μ that is introduced in minimal subtraction is the scale that makes the bare coupling dimensionless. As we have already mentioned, this is a regulating scale a priori, which has nothing to do with renormalization (denoting it as μ is not enough to qualify it as a renormalizaiton scale) and it is not clear how such a scale could control the renormalization group flow.

In this section, we first derive the minimal subtraction anomalous dimensions in the standard way, without paying much attention to these considerations. We then revisit the same calculations using a point of view more in line with the general discussion of the previous section. While making the minimal subtraction scheme fit the general picture, this point of view clarifies the true source of μ-dependence in this scheme and makes the determination of anomalous dimensions simpler and compatible with the formulas (B14) and (B23).

1. Standard derivation

From Eq. (C1) at one-loop order, because the factors $z_{X,ab}^{\overline{MS}}$ are constants and because the only source for μ-dependence is λ, we find

$$\gamma_X = \frac{\beta_\lambda/\lambda}{Z_X} \lambda \frac{z_{X,11}}{\epsilon}. \qquad \text{(C2)}$$

According to Eq. (B32) with $\Lambda = \mu$, β_λ/λ starts at order λ^0 with the contribution -2ϵ. To obtain the anomalous dimension at order λ, we just need to keep this leading contribution to β_λ/λ and replace Z_X by 1 in the denominator of Eq. (C2). One finds eventually

$$\gamma_X = -2z_{X,11}\lambda, \qquad \text{(C3)}$$

where we note that the ϵ coming from β_λ/λ has combined with the $1/\epsilon$ in (C2) to produce an order ϵ^0 anomalous dimension.

One can proceed similarly at two-loop order. Starting from Eq. (C1), one finds

$$\gamma_X = \frac{\beta_\lambda/\lambda}{Z_X} \left(\lambda \frac{z_{X,11}}{\epsilon} + 2\lambda^2 \frac{z_{X,22} + \epsilon z_{X,21}}{\epsilon^2} \right). \quad \text{(C4)}$$

This time, β_λ/λ (as well as Z_X) needs to be expanded to order λ. This includes the contribution -2ϵ but also γ_λ as given by Eq. (C3) with $X = \lambda$. One finds

$$\gamma_X = -4\lambda^2 \frac{z_{X,22} - z_{X,11}(z_{X,11} + z_{\lambda,11})/2}{\epsilon}$$
$$- (2z_{X,11}\lambda + 4z_{X,21}^{\overline{MS}}\lambda^2). \qquad \text{(C5)}$$

The finiteness of the beta function imposes that

$$z_{X,22} = \frac{1}{2}z_{X,11}(z_{X,11} + z_{\lambda,11}), \qquad \text{(C6)}$$

and we finally arrive at

$$\gamma_X = -(2z_{X,11}\lambda + 4z_{X,21}^{\overline{MS}}\lambda^2). \qquad \text{(C7)}$$

2. Connecting to the general discussion

Let us now re-derive these results with a slightly different perspective that makes the minimal subtraction fit the general discussion. In particular, Eqs. (C3) and (C7) will appear as particular cases of Eqs. (B14) and (B23).

Consider a slight generalization of the minimal subtraction scheme, which we refer to as $\Lambda\overline{MS}$, defined by the renormalization factors

$$Z_X^{\Lambda\overline{MS}} = 1 + \lambda \frac{z_{X,1}^{\Lambda\overline{MS}}}{\epsilon} + \lambda^2 \frac{z_{X,2}^{\Lambda\overline{MS}}}{\epsilon^2}, \qquad \text{(C8)}$$

with

$$z_{X,a}^{\Lambda\overline{MS}} = \left(\frac{\Lambda}{\mu} \right)^{2a\epsilon} z_{X,a}^{\overline{MS}}, \qquad \text{(C9)}$$

or, equivalently

$$z_{X,aa}^{\Lambda\overline{MS}} = z_{X,aa}^{\overline{MS}}, \qquad \text{(C10)}$$

$$z_{X,a(a-1)}^{\Lambda\overline{MS}} = z_{X,a(a-1)}^{\overline{MS}} + 2a z_{X,aa}^{\overline{MS}} \ln \frac{\Lambda}{\mu}, \quad \text{(C11)}$$
$$\cdots$$

where the dots represent $z_{X,ab}$ for $b < a - 1$. In fact, this defines a family of schemes parametrized by Λ, of which the standard minimal subtraction corresponds to the choice $\Lambda = \mu$. The scale Λ plays the role of the regulating scale, while the scale μ is the renormalization scale and the flow with respect to this latter scale needs to be determined for $m_B^2 = Z_{m^2}m^2$ and $\lambda_B = \Lambda^{2\epsilon}Z_\lambda\lambda$ fixed. In particular the anomalous dimensions should again be independent of the choice of Λ in the continuum limit (we will check this explicitly below), thus providing an alternative way to obtain the anomalous dimensions in minimal subtraction. The benefit of this approach is that, upon the appropriate introduction of Z_λ factors,

---

[13] The values of $z_{X,11}$ and $z_{X,22}$ are the same as in the previous section since they are scheme independent. On the other hand, $z_{X,10}^{\overline{MS}}$, $z_{X,1(-1)}^{\overline{MS}}$, $z_{X,21}^{\overline{MS}}$ and $z_{X,20}^{\overline{MS}}$ have no reason to be the same as those in the previous section.

the only way the coupling appears is via the combination $\Lambda^{2\epsilon} Z_\lambda \lambda$. Therefore one never needs to consider β_λ/λ and cancellations of the type $\epsilon \times 1/\epsilon$.

At one-loop order for instance, up to higher order corrections, one writes

$$Z_X = 1 + Z_\lambda \lambda \left(\frac{\Lambda}{\mu}\right)^{2\epsilon} \frac{z_{X,11}}{\epsilon}. \qquad (C12)$$

The only dependence on μ is via the factor $\mu^{-2\epsilon}$ and one obtains immediately

$$\gamma_X = -2z_{X,11} \frac{Z_\lambda}{Z_X} \lambda \left(\frac{\Lambda}{\mu}\right)^{2\epsilon} = -2z_{X,11} \lambda \left(\frac{\Lambda}{\mu}\right)^{2\epsilon}, (C13)$$

which boils down to (C3) in the continuum limit. Similarly, at two-loop order, one would write

$$
\begin{aligned}
Z_X &= 1 + \lambda \left(\frac{\Lambda}{\mu}\right)^{2\epsilon} \frac{z_{X,11}}{\epsilon} \\
&+ \lambda^2 \left(\frac{\Lambda}{\mu}\right)^{4\epsilon} \left(\frac{z_{X,22}}{\epsilon^2} + \frac{z_{X,21}}{\epsilon}\right) \\
&= 1 + Z_\lambda \lambda \left(\frac{\Lambda}{\mu}\right)^{2\epsilon} \frac{z_{X,11}}{\epsilon} \\
&+ Z_\lambda^2 \lambda^2 \left(\frac{\Lambda}{\mu}\right)^{4\epsilon} \left(\frac{z_{X,22} - z_{X,11}z_{\lambda,11}}{\epsilon^2} + \frac{z_{X,21}}{\epsilon}\right).
\end{aligned}
$$
$$(C14)$$

Again, the only μ-dependence is via the factors $\mu^{-2a\epsilon}$ and one recovers (C7) together with the constraint (C6). In fact, with this approach, it is not difficult to see that the minimal subtraction anomalous dimension is given at any order by

$$\gamma_X = -\sum_{a\geq 1} 2^a z_{X,a1}^{\overline{MS}} g^{2a}. \qquad (C15)$$

We mention also that the $\Lambda\overline{MS}$-scheme is no different from the generic schemes considered in the previous section and, as such, the expressions (C3) and (C7) should be compatible with (B14) and (B23). This is easily seen after noting that, from (C9), the μ-dependence of the factors $z_{X,a}^{\Lambda\overline{MS}}$ is controlled by the same equation that controls the Λ-dependence, see Eq. (B27), up to a sign:

$$\frac{\partial z_{X,a}^{\Lambda\overline{MS}}}{\partial \ln \mu} + 2a\epsilon z_{X,a}^{\Lambda\overline{MS}} = 0. \qquad (C16)$$

This in turn implies

$$\frac{\partial z_{X,ab}^{\Lambda\overline{MS}}}{\partial \ln \mu} = -2a z_{X,a(b+1)}^{\Lambda\overline{MS}}. \qquad (C17)$$

Using these identities, it is easily seen that, in the minimal subtraction scheme, (C3) and (C7) are compatible with (B14) and (B23). Moreover, the identity (B22) is nothing but a rewriting of (C6).

The present discussion also clarifies the true source of μ-dependence within the standard minimal subtraction scheme. By revisiting the derivation (C14) with $\Lambda = \mu$, we see that the scale μ that appears in the numerator of the factor $(\mu/\mu)^\epsilon$, and that stems from the rescaling of the coupling, has nothing to do with the RG running. The running originates instead from the scale μ that appears in the denominator of the factor $(\mu/\mu)^\epsilon$. Contrary to the former which is nothing but a regulating scale needed to make the coupling dimensionless in dimensional regularization, this second occurrence of μ is the renormalization scale. It is introduced here not by renormalization conditions, but rather by the minimal subtraction requirement that the renormalization factors do not depend explicitly on any scale and in particular on the regulating scale.

3. Integrating the one-loop flow

For completeness, let us recall here how the minimal subtraction beta functions and anomalous dimensions are integrated out at one- and two-loop orders. At one-loop order, we have

$$\frac{\beta_\lambda}{\lambda} = -\gamma_\lambda = 2z_{\lambda,11}\lambda. \qquad (C18)$$

This is rewritten as

$$\frac{d\lambda}{\lambda^2} = z_{\lambda,11} \, d\ln\mu^2, \qquad (C19)$$

which integrates to

$$\lambda(\mu) = \frac{\lambda_0}{1 - z_{\lambda,11}\lambda_0 \ln \frac{\mu^2}{\mu_0^2}} = \frac{1}{-z_{\lambda,11}\ln \frac{\mu^2}{\Lambda_{\text{LP}}^2}} \quad (C20)$$

with

$$\Lambda_{\text{LP}}^2 = \mu_0^2 \exp\left(\frac{1}{z_{\lambda,11}\lambda_0}\right). \qquad (C21)$$

The scale Λ_{LP} is the Landau pole and, if $z_{\lambda,11}$ is negative, the flow makes sense only for $\mu > \Lambda_{\text{LP}}$. We restrict to this case from now on.

Next, we write

$$\frac{\beta_m^2/m^2}{\beta_\lambda/\lambda} = \frac{\gamma_{m^2}}{\gamma_\lambda} = \frac{z_{m^2,11}}{z_{\lambda,11}}, \qquad (C22)$$

which is nothing but

$$d\ln m^2 = \frac{z_{m^2,11}}{z_{\lambda,11}} \, d\ln\lambda = d\ln(\lambda)^{\frac{z_{m^2,11}}{z_{\lambda,11}}}. \qquad (C23)$$

It follows that

$$\frac{m^2}{m_0^2} = \left(\frac{\lambda}{\lambda_0}\right)^{\frac{z_{m^2,11}}{z_{\lambda,11}}}. \qquad (C24)$$

Finally, we write

$$\frac{\gamma_\varphi}{\beta_\lambda/\lambda} = -\frac{\gamma_\varphi}{\gamma_\lambda} = -\frac{z_{\varphi,11}}{z_{\lambda,11}}, \qquad (C25)$$

which is nothing but

$$d \ln z_i = -\frac{z_{\varphi_i,11}}{z_{\lambda,11}} d \ln \lambda = d \ln(\lambda)^{-\frac{z_{\varphi_i,11}}{z_{\lambda,11}}}, \quad \text{(C26)}$$

where z_i is the rescaling factor (B3). It follows that

$$z_i(\mu, \mu_0) = \left(\frac{\lambda}{\lambda_0}\right)^{-\frac{z_{\varphi,11}}{z_{\lambda,11}}}. \quad \text{(C27)}$$

4. Integrating the two-loop flow

We have

$$\frac{\beta_\lambda}{\lambda} = -\gamma_\lambda = 2z_{\lambda,11}\lambda + 4z_{\lambda,21}\lambda^2, \quad \text{(C28)}$$

which is nothing but

$$\frac{d\lambda}{\lambda^2 \left(1 + 2\frac{z_{\lambda,21}}{z_{\lambda,11}}\lambda\right)} = z_{\lambda,11} d \ln \mu^2. \quad \text{(C29)}$$

We can rewrite this conveniently as

$$z_{\lambda,11} d \ln \mu^2 = -\frac{\frac{1}{\lambda}}{\left(\frac{1}{\lambda} + 2\frac{z_{\lambda,21}}{z_{\lambda,11}}\right)} d\left(\frac{1}{\lambda}\right)$$

$$= \left[-1 + \frac{2\frac{z_{\lambda,21}}{z_{\lambda,11}}}{\frac{1}{\lambda} + 2\frac{z_{\lambda,21}}{z_{\lambda,11}}}\right] d\left(\frac{1}{\lambda}\right), \quad \text{(C30)}$$

which integrates to

$$z_{\lambda,11} \ln \frac{\mu^2}{\mu_0^2} = \frac{1}{\lambda_0} - \frac{1}{\lambda(\mu)} + 2\frac{z_{\lambda,21}}{z_{\lambda,11}} \ln \frac{\frac{1}{\lambda(\mu)} + 2\frac{z_{\lambda,21}}{z_{\lambda,11}}}{\frac{1}{\lambda_0} + 2\frac{z_{\lambda,21}}{z_{\lambda,11}}}, \quad \text{(C31)}$$

and gives μ as a function of λ. We notice that, because the running of g is logarithmic, the second term is subleading in the UV and we recover the one-loop running.

We can estimate the correction to the one-loop behavior by replacing $\lambda(\mu)$ by $\lambda_{\text{1loop}}(\mu)$ in the logarithm. We obtain

$$\frac{1}{\lambda(\mu)} = \frac{1}{\lambda_0} - z_{\lambda,11} \ln \frac{\mu^2}{\mu_0^2} + 2\frac{z_{\lambda,21}}{z_{\lambda,11}} \ln \frac{-z_{\lambda,11} \ln \frac{\mu^2}{\mu_0^2}}{\frac{1}{\lambda_0} + 2\frac{z_{\lambda,21}}{z_{\lambda,11}}}. \quad \text{(C32)}$$

We note that

$$\lambda_{\text{2loop}} - \lambda_{\text{1loop}} = -2\lambda_{\text{1loop}}\lambda_{\text{2loop}}\frac{z_{\lambda,21}}{z_{\lambda,11}} \ln \frac{-z_{\lambda,11} \ln \frac{\mu^2}{\mu_0^2}}{\frac{1}{\lambda_0} + 2\frac{z_{\lambda,21}}{z_{\lambda,11}}}, \quad \text{(C33)}$$

and thus the corrections are not that small. We mention also that (C31) provides corrections to the Landau pole defined by the scale at which $1/\lambda(\mu)$ vanishes. One finds

$$\Lambda_{\text{LP}}^2 = \mu_0^2 \left(\frac{1}{1 + \frac{z_{\lambda,11}}{2z_{\lambda,21}\lambda_0}}\right)^{2\frac{z_{\lambda,21}}{z_{\lambda,11}^2}} \exp\left(\frac{1}{z_{\lambda,11}\lambda_0}\right) \quad \text{(C34)}$$

in terms of which we have

$$z_{\lambda,11} \ln \frac{\mu^2}{\Lambda_{\text{LP}}^2} = -\frac{1}{\lambda(\mu)} + 2\frac{z_{\lambda,21}}{z_{\lambda,11}} \ln \left(1 + \frac{z_{\lambda,11}}{2z_{\lambda,21}} \frac{1}{\lambda(\mu)}\right). \quad \text{(C35)}$$

Next, we write

$$\frac{\beta_{m^2}}{m^2} = -\gamma_{m^2} = 2z_{m^2,11}\lambda + 4z_{m^2,21}\lambda^2, \quad \text{(C36)}$$

which is nothing but

$$d \ln m^2 = \left(z_{m^2,11}\lambda + 2z_{m^2,21}\lambda^2\right) d \ln \mu^2. \quad \text{(C37)}$$

Upon using (C30), this is rewritten as

$$z_{\lambda,11} d \ln m^2 = -\frac{z_{m^2,11} + 2z_{m^2,21}\lambda}{\frac{1}{\lambda} + 2\frac{z_{\lambda,21}}{z_{\lambda,11}}} d\left(\frac{1}{\lambda}\right) = -\left[\frac{z_{m^2,11}}{\frac{1}{\lambda} + 2\frac{z_{\lambda,21}}{z_{\lambda,11}}} + \frac{2z_{m^2,21}}{\frac{1}{\lambda}\left(\frac{1}{\lambda} + 2\frac{z_{\lambda,21}}{z_{\lambda,11}}\right)}\right] d\left(\frac{1}{\lambda}\right)$$

$$= -\left[\frac{z_{m^2,11}}{\frac{1}{\lambda} + 2\frac{z_{\lambda,21}}{z_{\lambda,11}}} + \frac{z_{\lambda,11}}{z_{\lambda,21}} z_{m^2,21} \left(\frac{1}{\frac{1}{\lambda}} - \frac{1}{\frac{1}{\lambda} + 2\frac{z_{\lambda,21}}{z_{\lambda,11}}}\right)\right] d\left(\frac{1}{\lambda}\right), \quad \text{(C38)}$$

which is easily integrated to

$$\ln \frac{m^2}{m_0^2} = \frac{z_{m^2,21}}{z_{\lambda,21}} \ln \frac{\lambda}{\lambda_0} + \left(\frac{z_{m^2,21}}{z_{\lambda,21}} - \frac{z_{m^2,11}}{z_{\lambda,11}}\right) \ln \frac{\frac{1}{\lambda(\mu)} + 2\frac{z_{\lambda,21}}{z_{\lambda,11}}}{\frac{1}{\lambda_0} + 2\frac{z_{\lambda,21}}{z_{\lambda,11}}}$$

$$= \frac{z_{m^2,11}}{z_{\lambda,11}} \ln \frac{\lambda}{\lambda_0} + \left(\frac{z_{m^2,21}}{z_{\lambda,21}} - \frac{z_{m^2,11}}{z_{\lambda,11}}\right) \ln \frac{1 + 2\frac{z_{\lambda,21}}{z_{\lambda,11}}\lambda}{1 + 2\frac{z_{\lambda,21}}{z_{\lambda,11}}\lambda_0}, \quad \text{(C39)}$$

or

$$\frac{m^2}{m_0^2} = \left(\frac{\lambda}{\lambda_0}\right)^{\frac{z_{m^2,11}}{z_{\lambda,11}}} \left(\frac{1 + 2\frac{z_{\lambda,21}}{z_{\lambda,11}}\lambda}{1 + 2\frac{z_{\lambda,21}}{z_{\lambda,11}}\lambda_0}\right)^{\frac{z_{\lambda,11}z_{m^2,21} - z_{m^2,11}z_{\lambda,21}}{z_{\lambda,21}z_{\lambda,11}}} . \tag{C40}$$

The second factor approaches 1 in the deep UV and we recover the one-loop running.

Finally, if we solve formally (C28) and (C36) for λ and λ^2, we find

$$\lambda = \frac{\frac{\beta_\lambda}{\lambda}z_{m^2,21} - \frac{\beta_{m^2}}{m^2}z_{\lambda,21}}{2(z_{\lambda,11}z_{m^2,21} - z_{m^2,11}z_{\lambda,21})} \quad \text{and} \quad \lambda^2 = \frac{\frac{\beta_{m^2}}{m^2}z_{\lambda,11} - \frac{\beta_\lambda}{\lambda}z_{m^2,11}}{4(z_{\lambda,11}z_{m^2,21} - z_{m^2,11}z_{\lambda,21})} . \tag{C41}$$

Plugging this back into

$$\gamma_{\varphi_i} = 2z_{\varphi_i,11}\lambda + 4z_{\varphi_i,21}\lambda^2 , \tag{C42}$$

gives

$$\gamma_\varphi = -\frac{z_{\varphi,11}z_{m^2,21} - z_{m^2,11}z_{\varphi,21}}{z_{\lambda,11}z_{m^2,21} - z_{m^2,11}z_{\lambda,21}}\frac{\beta_\lambda}{\lambda}$$
$$- \frac{z_{\varphi,11}z_{\lambda,21} - z_{\lambda,11}z_{\varphi,21}}{z_{m^2,11}z_{\lambda,21} - z_{\lambda,11}z_{m^2,21}}\frac{\beta_{m^2}}{m^2} \tag{C43}$$

from which it follows that

$$z_i(\mu, \mu_0) = \left(\frac{\lambda}{\lambda_0}\right)^{-\frac{z_{\varphi,11}z_{m^2,21} - z_{m^2,11}z_{\varphi,21}}{z_{\lambda,11}z_{m^2,21} - z_{m^2,11}z_{\lambda,21}}}$$
$$\times \left(\frac{m^2}{m_0^2}\right)^{-\frac{z_{\varphi,11}z_{\lambda,21} - z_{\lambda,11}z_{\varphi,21}}{z_{m^2,11}z_{\lambda,21} - z_{\lambda,11}z_{m^2,21}}} . \tag{C44}$$

To recover the one-loop behavior, we notice that deep in the UV, Eq. (C24) holds, and this leads to

$$z(\mu, \mu_0) = \left(\frac{\lambda}{\lambda_0}\right)^{-\frac{z_{\varphi,11}z_{m^2,21} - z_{m^2,11}z_{\varphi,21}}{z_{\lambda,11}z_{m^2,21} - z_{m^2,11}z_{\lambda,21}}}$$
$$\times \left(\frac{\lambda}{\lambda_0}\right)^{-\frac{z_{m^2,11}}{z_{\lambda,11}}\frac{z_{\varphi,11}z_{\lambda,21} - z_{\lambda,11}z_{\varphi,21}}{z_{m^2,11}z_{\lambda,21} - z_{\lambda,11}z_{m^2,21}}} . \tag{C45}$$

We notice that the terms proportional to $z_{\varphi,21}$ in the numerator of the exponent cancel and we are left with

$$z_i(\mu, \mu_0) = \left(\frac{\lambda}{\lambda_0}\right)^{-\frac{z_{\varphi,11}\left(z_{m^2,21} - \frac{z_{\lambda,21}}{z_{\lambda,11}}z_{m^2,11}\right)}{z_{\lambda,11}z_{m^2,21} - z_{m^2,11}z_{\lambda,21}}}$$
$$= \left(\frac{\lambda}{\lambda_0}\right)^{-\frac{z_{\varphi,11}}{z_{\lambda,11}}} , \tag{C46}$$

in agreement with Eq. (C27).

We mention that the previous derivation is not valid for a massless field and the formula (C44) is plagued by singularities (since $z_{m^2,ab} = 0$). However, plugging (C40) into (C44), we can combine the various powers of λ/λ_0 just as before and we arrive at

$$z_i(\mu, \mu_0) = \left(\frac{\lambda}{\lambda_0}\right)^{-\frac{z_{\varphi,11}}{z_{\lambda,11}}} \left(\frac{1 + 2\frac{z_{\lambda,21}}{z_{\lambda,11}}\lambda}{1 + 2\frac{z_{\lambda,21}}{z_{\lambda,11}}\lambda_0}\right)^{\frac{z_{\varphi,11}}{z_{\lambda,11}} - \frac{z_{\varphi,21}}{z_{\lambda,21}}} . \tag{C47}$$

These formulas do not make any reference to the mass of the fields and apply, therefore, to a massless field as well.

Appendix D: Asymptotic expansion in the UV

In this section, we collect the next-to-leading order UV and IR asymptotic expansions of the various two anomalous dimensions as computed in the IR-safe scheme. The corresponding expansions for the beta functions for λ and m^2 can be deduced from the non-renormalization theorems, whereas that for M can be deduced directly from its relation to γ_M.

In the UV, at next-to-leading order of the asymptotic expansion, we find for the gluon and ghost anomalous dimensions

$$\gamma_A = \lambda \left\{ \left[-\frac{13}{3} + \left(\frac{65}{4} + \frac{3}{2} \ln \frac{\mu^2}{m^2} \right) \frac{m^2}{\mu^2} \right] + \frac{N_f}{N} \left[\frac{4}{3} - 8 \frac{M^2}{\mu^2} \right] \right\}$$

$$+ \lambda^2 \left\{ -\frac{85}{6} + \left(\frac{18343}{96} + \frac{\pi^2}{48} + \frac{171}{4} \zeta(3) - \frac{891}{16} S_2 + \frac{205}{16} \ln \frac{\mu^2}{m^2} + \frac{35}{8} \ln^2 \frac{\mu^2}{m^2} \right) \frac{m^2}{\mu^2} \right.$$

$$+ \frac{N_f}{N} \left[\frac{17}{3} - \left(\frac{8}{3} + 48\zeta(3) \right) \frac{m^2}{\mu^2} - \left(\frac{281}{3} + 16\zeta(3) \right) \frac{M^2}{\mu^2} + 2 \left(\frac{m^2}{\mu^2} - 2 \left(1 + \frac{M^2}{m^2} \right) \frac{M^2}{\mu^2} \right) \tilde{I}_{mMM} \right.$$

$$+ \left(2 \ln \frac{\mu^2}{m^2} - 2 \ln \frac{\mu^2}{m^2} \ln \frac{\mu^2}{M^2} + \ln^2 \frac{\mu^2}{M^2} \right) \frac{m^2}{\mu^2} - 2 \left(\ln \frac{\mu^2}{m^2} + 2 \ln \frac{\mu^2}{M^2} \right) \frac{M^2}{\mu^2} \right]$$

$$+ \left. \frac{N_f}{N} \frac{C_F}{N} \left[4 - \left(\frac{128}{3} - 32\zeta(3) \right) \frac{m^2}{\mu^2} - 48 \frac{M^2}{\mu^2} \right] \right\} , \tag{D1}$$

$$\gamma_c = \lambda \left\{ -\frac{3}{2} - \left(\frac{3}{4} - \frac{3}{2} \ln \frac{\mu^2}{m^2} \right) \frac{m^2}{\mu^2} \right\}$$

$$+ \lambda^2 \left\{ -\frac{17}{4} + \left(-\frac{211}{8} + \frac{\pi^2}{48} + \frac{3}{4} \zeta(3) - \frac{891}{16} S_2 + \frac{103}{8} \ln \frac{\mu^2}{m^2} + \frac{35}{8} \ln^2 \frac{\mu^2}{m^2} \right) \frac{m^2}{\mu^2} \right.$$

$$+ \frac{N_f}{N} \left[\frac{1}{2} + \frac{3}{2} \frac{m^2}{\mu^2} + 11 \frac{M^2}{\mu^2} + 2 \left(\frac{m^2}{\mu^2} - 2 \left(1 + \frac{M^2}{m^2} \right) \frac{M^2}{\mu^2} \right) \tilde{I}_{mMM} \right.$$

$$+ \left. \left. \left(\ln \frac{\mu^2}{m^2} - 2 \ln \frac{\mu^2}{m^2} \ln \frac{\mu^2}{M^2} + \ln^2 \frac{\mu^2}{M^2} \right) \frac{m^2}{\mu^2} - 2 \left(\ln \frac{\mu^2}{m^2} + 2 \ln \frac{\mu^2}{M^2} \right) \frac{M^2}{\mu^2} \right] \right\} , \tag{D2}$$

with

$$S_2 \equiv \frac{4}{9\sqrt{3}} \operatorname{Im} \operatorname{Li}_2(e^{i\pi/3}) , \tag{D3}$$

and

$$\tilde{I}_{mMM} = -m \operatorname{Re} \left\{ \frac{\sqrt{m^2 - 4M^2}}{m^2 - 4M^2} \left[\frac{\pi^2}{6} - \frac{1}{2} \ln^2 \frac{M^2}{m^2} + \ln^2 \left(\frac{1}{2} - \frac{\sqrt{m^2 - 4M^2}}{2m} \right) - 2\operatorname{Li}_2 \left(\frac{1}{2} - \frac{\sqrt{m^2 - 4M^2}}{2m} \right) \right] \right\} , \tag{D4}$$

where Li_2 denotes the dilogarithm function. It is easily checked that the term between square brackets in $\tilde{I}_{mMM}$ vanishes linearly as $m \to 2M$ and thus the above expressions for γ_A and γ_c are regular in this limit.

In mass-independent schemes, the coupling beta function is two-loop universal, whereas in mass-dependent schemes, such as the IR-safe scheme considered here, it is two-loop universal in the UV. Using $\beta_\lambda/\lambda = \gamma_A + 2\gamma_c$, we have checked that we recover indeed the two-loop univeral behavior in the UV [75].

Similarly, for the quark anomalous dimensions, we find

$$\gamma_\psi = \lambda \frac{C_F}{N} \left(\frac{9}{2} - 3 \ln \frac{\mu^2}{m^2} \right) \frac{m^2}{\mu^2}$$

$$+ \lambda^2 \frac{C_F}{N} \left\{ \frac{25}{2} + \left(\frac{695}{8} - \frac{\pi^2}{24} - 45\zeta(3) + \frac{891}{8} S_2 - \frac{47}{2} \ln \frac{\mu^2}{m^2} - \frac{35}{4} \ln^2 \frac{\mu^2}{m^2} \right) \frac{m^2}{\mu^2} - \left(31 - 18\zeta(3) \right) \frac{M^2}{\mu^2} \right.$$

$$+ \frac{C_F}{N} \left[-3 - 8 \left(5 - 6\zeta(3) \right) \frac{m^2}{\mu^2} + 24 \frac{M^2}{\mu^2} \right]$$

$$+ \frac{N_f}{N} \left[-2 - 5 \frac{m^2}{\mu^2} - 18 \frac{M^2}{\mu^2} - 4 \left(\frac{m^2}{\mu^2} - 2 \left(1 + \frac{M^2}{m^2} \right) \frac{M^2}{\mu^2} \right) \tilde{I}_{mMM} \right.$$

$$- \left. \left. 2 \left(\ln \frac{\mu^2}{m^2} - 2 \ln \frac{\mu^2}{m^2} \ln \frac{\mu^2}{M^2} + \ln^2 \frac{\mu^2}{M^2} \right) \frac{m^2}{\mu^2} + 4 \left(\ln \frac{\mu^2}{m^2} + 2 \ln \frac{\mu^2}{M^2} \right) \frac{M^2}{\mu^2} \right] \right\} , \tag{D5}$$

and

$$
\begin{aligned}
\gamma_M = {} & \lambda \frac{C_F}{N} \left\{ 6 - \left(\frac{9}{2} + 3\ln\frac{\mu^2}{m^2} \right) \frac{m^2}{\mu^2} - 6\frac{M^2}{\mu^2}\ln\frac{\mu^2}{M^2} \right\} \\
& + \lambda^2 \frac{C_F}{N} \left\{ \frac{67}{2} - \left(\frac{41}{2} + \frac{\pi^2}{24} + 69\zeta(3) - \frac{891}{8}S_2 + \frac{49}{4}\ln\frac{\mu^2}{m^2} + \frac{35}{4}\ln^2\frac{\mu^2}{m^2} \right) \frac{m^2}{\mu^2} + \left(3 - 36\zeta(3) - 46\ln\frac{\mu^2}{M^2} \right) \frac{M^2}{\mu^2} \right. \\
& \qquad\qquad + \frac{C_F}{N} \left[3 - \left(\frac{35}{2} - 48\zeta(3) \right) \frac{m^2}{\mu^2} + 2\left(7 - 12\zeta(3) \right) \frac{M^2}{\mu^2} - 72\tilde{I}_{mMM}\frac{M^2}{\mu^2} \right. \\
& \qquad\qquad\qquad\qquad \left. - 45\ln\frac{\mu^2}{m^2}\frac{m^2}{\mu^2} + 18\left(3 - 2\ln\frac{\mu^2}{M^2} \right)\ln\frac{\mu^2}{M^2}\frac{M^2}{\mu^2} \right] \\
& \qquad\qquad + \frac{N_f}{N} \left[-2 + 5\frac{m^2}{\mu^2} - 10\frac{M^2}{\mu^2} - 4\left(\frac{m^2}{\mu^2} - 2\left(1 + \frac{M^2}{m^2} \right)\frac{M^2}{\mu^2} \right)\tilde{I}_{mMM} \right. \\
& \qquad\qquad\qquad\qquad \left.\left. - 2\left(\ln\frac{\mu^2}{m^2} - 2\ln\frac{\mu^2}{m^2}\ln\frac{\mu^2}{M^2} + \ln^2\frac{\mu^2}{M^2} \right)\frac{m^2}{\mu^2} + 4\left(\ln\frac{\mu^2}{m^2} + 3\ln\frac{\mu^2}{M^2} \right)\frac{M^2}{\mu^2} \right] \right\} .
\end{aligned}
\tag{D6}
$$

Appendix E: Asymptotic expansion in the IR

In order to obtain the IR asymptotic expansion of the two-loop anomalous dimensions at next-to-leading order, we first checked that all the master integrals required to obtain the anomalous dimensions to order μ^4/m^4 and μ^4/M^4 are either known analytically or such that one can always root the external momentum through massive propagators. For this second type of master integrals, one can employ the strategy of Ref. [72] that we briefly reviewed in Sec. III D 3. For completeness, we here provide the resulting expansions.

In the case of S_{abc}, assuming $a \neq 0$, it is convenient to choose the loop momenta as follows

$$
S_{abc}(k) = \int_p \int_q \frac{1}{(p+k)^2 + a} \frac{1}{(q+p)^2 + b} \frac{1}{q^2 + c} .
\tag{E1}
$$

One can then expand the massive propagator carrying the external momentum k:

$$
\frac{1}{(p+k)^2 + a} = \sum_{n=0}^{\infty} (-1)^n \frac{(2(p\cdot k) + k^2)^n}{(p^2 + a)^{n+1}} = \sum_{n=0}^{\infty} (-1)^n \sum_{\ell=0}^{n} \frac{n!}{\ell!(n-\ell)!} \frac{(2(p\cdot k))^\ell (k^2)^{n-\ell}}{(p^2 + a)^{n+1}} .
\tag{E2}
$$

This yields

$$
S_{abc}(k) = \sum_{n=0}^{\infty} (-1)^n \sum_{\ell=0}^{n} \frac{n!}{\ell!(n-\ell)!} \int_p \int_q \frac{(2p\cdot k)^\ell (k^2)^{n-\ell}}{(p^2 + a)^{n+1}} \frac{1}{(q+p)^2 + b} \frac{1}{q^2 + c} .
\tag{E3}
$$

The p-integral vanishes for ℓ odd, whereas for ℓ even, one can use the formula

$$
\int \frac{d^d p}{(2\pi)^d} f(p^2)\,(2\,p\cdot k)^\ell = \frac{\ell!}{(\ell/2)!} \frac{(k^2)^{\ell/2}}{(d/2)_{\ell/2}} \int \frac{d^d p}{(2\pi)^d} f(p^2)\,(p^2)^{\ell/2} ,
\tag{E4}
$$

given in Ref. [71], where $(a)_n \equiv a(a+1)\cdots(a+n-1)$ is the Pochhammer symbol. One then arrives at

$$
\begin{aligned}
S_{abc}(k) &= \sum_{n=0}^{\infty} (-1)^n \sum_{\ell=0}^{[n/2]} \frac{n!}{\ell!(n-2\ell)!} \frac{(k^2)^{n-\ell}}{(d/2)_\ell} \int_p \int_q \frac{(p^2)^\ell}{(p^2 + a)^{n+1}} \frac{1}{(q+p)^2 + b} \frac{1}{q^2 + c} \\
&= \sum_{n=0}^{\infty} \sum_{\ell=0}^{[n/2]} \sum_{h=0}^{\ell} (-1)^{n+\ell-h} \frac{n!}{(n-2\ell)!h!(\ell-h)!} \frac{(k^2)^{n-\ell}}{(d/2)_\ell} a^{\ell-h} I_{(n+1-h)11}(a,b,c),
\end{aligned}
\tag{E5}
$$

where we redefined $\ell \to 2\ell$ (since it is even) and $[n/2]$ denotes the integer part of $n/2$.

We have thus expressed the IR expansion of S_{abc} in terms of the integrals $I_{(n+1-h)11}$ which are essentially nothing but multiple derivative of $I_{111}(a,b,c)$ with respect to a. These multiple derivatives can be conveniently obtained by

repeated use of Eq. (56).[14] We note that $\ell \leq n/2$ and thus the exponent of k^2 in (E5) is such that $n - \ell \geq n/2$. This implies that terms with $n > 2p$ contribute to powers of k^2 with an exponent strictly larger than p. In other words, to obtain the expansion up to order $(k^2)^p$, it is enough to truncate the sum over n up to and including $n = 2p$.

In the case of $U_{abcd}(k)$, assuming $a \neq 0$, we write

$$U_{abcd}(k) = \int_p \int_q \frac{1}{(p+k)^2 + a} \frac{1}{p^2 + b} \frac{1}{q^2 + c} \frac{1}{(q+p)^2 + d}, \tag{E6}$$

which is similar to (E1) with $b \to d$ and an additional propagator $1/(p^2 + b)$. It is then clear that by using the same technique as above, we arrive at

$$U_{abcd}(k) = \sum_{n=0}^{\infty} (-1)^n \sum_{\ell=0}^{[n/2]} \frac{n!}{\ell!(n-2\ell)!} \frac{(k^2)^{n-\ell}}{(d/2)_\ell} \int_p \int_q \frac{(p^2)^\ell}{(p^2+a)^{n+1}} \frac{1}{p^2 + b} \frac{1}{q^2 + c} \frac{1}{(q+p)^2 + d}$$

$$= \sum_{n=0}^{\infty} \sum_{\ell=0}^{[n/2]} \sum_{h=0}^{\ell} (-1)^{n+\ell-h} \frac{n!}{(n-2\ell)!h!(\ell-h)!} \frac{(k^2)^{n-\ell}}{(d/2)_\ell} a^{\ell-h}$$

$$\times \int_p \int_q \frac{1}{(p^2+a)^{n+1-h}} \frac{1}{p^2 + b} \frac{1}{q^2 + c} \frac{1}{(q+p)^2 + d}. \tag{E7}$$

In the case where $a = b$, we then obtain

$$U_{aacd}(k) = \sum_{n=0}^{\infty} \sum_{\ell=0}^{[n/2]} \sum_{h=0}^{\ell} (-1)^{n+\ell-h} \frac{n!}{(n-2\ell)!h!(\ell-h)!} \frac{(k^2)^{n-\ell}}{(d/2)_\ell} a^{\ell-h} I_{(n+2-h)11}(a,c,d). \tag{E8}$$

In the case $a \neq b$, we write

$$\alpha_{n+1} \equiv \frac{1}{(p^2+a)^{n+1}} \frac{1}{p^2+b} = \frac{1}{(p^2+a)^n} \frac{1}{p^2+a} \frac{1}{p^2+b} = \frac{1}{b-a} \frac{1}{(p^2+a)^n} \left[\frac{1}{p^2+a} - \frac{1}{p^2+b} \right]$$

$$= \frac{1}{b-a} \frac{1}{(p^2+a)^{n+1}} - \frac{1}{b-a} \alpha_n = \frac{1}{b-a} \frac{1}{(p^2+a)^{n+1}} - \frac{1}{(b-a)^2} \frac{1}{(p^2+a)^n} + \frac{1}{(b-a)^2} \alpha_{n-1}$$

$$= \frac{1}{b-a} \frac{1}{(p^2+a)^{n+1}} - \frac{1}{(b-a)^2} \frac{1}{(p^2+a)^n} + \cdots + \frac{(-1)^n}{(b-a)^{n+1}} \frac{1}{p^2+a} - \frac{(-1)^n}{(b-a)^{n+1}} \alpha_0$$

$$= \sum_{j=0}^{n} \frac{(-1)^j}{(b-a)^{j+1}} \frac{1}{(p^2+a)^{n+1-j}} - \frac{(-1)^n}{(b-a)^{n+1}} \frac{1}{p^2+b}, \tag{E9}$$

and then

$$U_{abcd}(k) = -\sum_{n=0}^{\infty} \sum_{\ell=0}^{[n/2]} \sum_{h=0}^{\ell} (-1)^\ell \frac{n!}{(n-2\ell)!h!(\ell-h)!} \frac{(k^2)^{n-\ell}}{(d/2)_\ell} \frac{a^{\ell-h}}{(b-a)^{n+1-h}} I_{111}(b,c,d)$$

$$+ \sum_{n=0}^{\infty} \sum_{\ell=0}^{[n/2]} \sum_{h=0}^{\ell} \sum_{j=0}^{n-h} (-1)^{n+\ell-h+j} \frac{n!}{(n-2\ell)!h!(\ell-h)!} \frac{(k^2)^{n-\ell}}{(d/2)_\ell} \frac{a^{\ell-h}}{(b-a)^{j+1}} I_{(n+1-h-j)11}(a,c,d). \tag{E10}$$

As before, to obtain the expansion up to order $(k^2)^p$, we need to consider the sum over n up to $n = 2p$.

Let us finally consider the case of M_{abcde}, assuming $a \neq 0$ and $b \neq 0$. We write

$$M_{abcde}(k) = \int_p \int_q \frac{1}{(p+k)^2 + a} \frac{1}{(q+k)^2 + b} \frac{1}{p^2 + c} \frac{1}{q^2 + d} \frac{1}{(p-q)^2 + e}, \tag{E11}$$

---

[14] One could wonder why it is not possible to simply take multiple derivative of the explicit expression for $I_{111}(a,b,c)$. Although possible this leads to cumbersome combinations of hypergeometric functions and their derivatives. It is much more convenient to first express the multiple derivatives algebraically in terms of $I_{111}(a,b,c)$ using Eq. (56) and only then do the substitution of $I_{111}(a,b,c)$ by its explicit expression.

where we assume $a \neq 0$ and $b \neq 0$. The expansion of the two propagators carrying k leads to

$$M_{abcde}(k) = \sum_{n_1=0}^{\infty} \sum_{n_2=0}^{\infty} \sum_{\ell_1=0}^{n_1} \sum_{\ell_2=0}^{n_2} \frac{(-1)^{n_1+n_2} n_1! n_2!}{\ell_1! \ell_2! (n_1-\ell_1)! (n_2-\ell_2)!} (k^2)^{n_1+n_2-\ell_1-\ell_2}$$
$$\times \int_p \int_q \frac{(2(p\cdot k))^{\ell_1}}{(p^2+a)^{n_1+1}} \frac{(2(q\cdot k))^{\ell_2}}{(q^2+b)^{n_2+1}} \frac{1}{p^2+c} \frac{1}{q^2+d} \frac{1}{(p-q)^2+e} \,. \tag{E12}$$

This can be simplified using the last formula in the Appendix of Ref. [71]

$$M_{abcde}(k) = \sum_{n_1=0}^{\infty} \sum_{n_2=0}^{\infty} \sum_{\ell_1=0}^{n_1} \sum_{\ell_2=0}^{n_2} \sum_{2h_{1/2}+h_3=\ell_{1/2}} \frac{(-1)^{n_1+n_2} n_1! n_2!}{(n_1-\ell_1)!(n_2-\ell_2)! h_1! h_2! h_3!} \frac{(k^2)^{n_1+n_2-(\ell_1+\ell_2)/2}}{(d/2)_{(\ell_1+\ell_2)/2}}$$
$$\times \int_p \int_q \frac{(p^2)^{h_1}}{(p^2+a)^{n_1+1}} \frac{(q^2)^{h_2}}{(q^2+b)^{n_2+1}} \frac{1}{p^2+c} \frac{1}{q^2+d} \frac{(2p\cdot q)^{h_3}}{(p-q)^2+e} \,. \tag{E13}$$

Using $2p\cdot q = p^2 + q^2 + e - (p-q)^2 - e$, this rewrites

$$M_{abcde}(k) = \sum_{n_1=0}^{\infty} \sum_{n_2=0}^{\infty} \sum_{\ell_1=0}^{n_1} \sum_{\ell_2=0}^{n_2} \sum_{2h_{1/2}+h_3=\ell_{1/2}} \sum_{j_1+j_2+j_3+j_4=h_3} \frac{(-1)^{n_1+n_2+j_4} n_1! n_2!}{(n_1-\ell_1)!(n_2-\ell_2)! h_1! h_2! j_1! j_2! j_3! j_4!}$$
$$\times \frac{(k^2)^{n_1+n_2-(\ell_1+\ell_2)/2}}{(d/2)_{(\ell_1+\ell_2)/2}} e^{j_3} \int_p \int_q \frac{(p^2)^{h_1+j_1}}{(p^2+a)^{n_1+1}} \frac{(q^2)^{h_2+j_2}}{(q^2+b)^{n_2+1}} \frac{1}{p^2+c} \frac{1}{q^2+d} \frac{1}{((p-q)^2+e)^{1-j_4}}$$
$$= \sum_{n_1=0}^{\infty} \sum_{n_2=0}^{\infty} \sum_{\ell_1=0}^{n_1} \sum_{\ell_2=0}^{n_2} \sum_{2h_{1/2}+h_3=\ell_{1/2}} \sum_{j_1+j_2+j_3+j_4=h_3} \sum_{p_1=0}^{h_1+j_1} \sum_{p_2=0}^{h_2+j_2}$$
$$\times \frac{(-1)^{n_1+n_2+j_4+h_1+j_1-p_1+h_2+j_2-p_2} n_1! n_2! (h_1+j_1)! (h_2+j_2)!}{(n_1-\ell_1)!(n_2-\ell_2)! h_1! h_2! j_1! j_2! j_3! j_4! p_1! p_2! (h_1+j_1-p_1)! (h_2+j_2-p_2)!} \frac{(k^2)^{n_1+n_2-(\ell_1+\ell_2)/2}}{(d/2)_{(\ell_1+\ell_2)/2}}$$
$$\times a^{h_1+j_1-p_1} b^{h_2+j_2-p_2} e^{j_3} \int_p \int_q \frac{(p^2+c)^{-1}}{(p^2+a)^{n_1+1-p_1}} \frac{(q^2+d)^{-1}}{(q^2+b)^{n_2+1-p_2}} \frac{1}{((p-q)^2+e)^{1-j_4}} \,. \tag{E14}$$

In the case $a=c$ and $b=d$, we arrive at

$$M_{ababe}(k) = \sum_{n_1=0}^{\infty} \sum_{n_2=0}^{\infty} \sum_{\ell_1=0}^{n_1} \sum_{\ell_2=0}^{n_2} \sum_{2h_{1/2}+h_3=\ell_{1/2}} \sum_{j_1+j_2+j_3+j_4=h_3} \sum_{p_1=0}^{h_1+j_1} \sum_{p_2=0}^{h_2+j_2}$$
$$\times \frac{(-1)^{n_1+n_2+j_4+h_1+j_1-p_1+h_2+j_2-p_2} n_1! n_2! (h_1+j_1)! (h_2+j_2)!}{(n_1-\ell_1)!(n_2-\ell_2)! h_1! h_2! j_1! j_2! j_3! j_4! p_1! p_2! (h_1+j_1-p_1)! (h_2+j_2-p_2)!}$$
$$\times \frac{(k^2)^{n_1+n_2-(\ell_1+\ell_2)/2}}{(d/2)_{(\ell_1+\ell_2)/2}} a^{h_1+j_1-p_1} b^{h_2+j_2-p_2} e^{j_3} I_{(n_1+2-p_1)(n_2+2-p_2)(1-j_4)}(a,b,e) \,. \tag{E15}$$

In the other cases, we need to make use of (E9). We note that $\ell_i \leq n_i$ and thus $n_i - \ell_i/2 \geq n_i/2$, so terms with $n_1 + n_2 > 2p$ contribute to powers of k^2 with exponent $n_1 + n_2 - (\ell_1 + \ell_2)/2 > p$. In other words, to obtain the expansion up to order $(k^2)^p$, we need to truncate the double sum over n_1 and n_2 such that it includes all terms with $n_1 + n_2 \leq 2p$. For $j_4 = 0$, we need to relate $I_{(n_1+2-p_1)(n_2+2-p_2)1}(a,b,e)$ to $I_{111}(a,b,e)$ by repeated use of (56). For $j_4 \geq 1$, we can relate $I_{(n_1+2-p_1)(n_2+2-p_2)(1-j_4)}(a,b,e)$ to

$$J_{\alpha,\beta}(a) \equiv \int_p \frac{1}{(p^2+a)^{\alpha}(p^2)^{\beta}} = \frac{a^{2-\alpha-\beta-\epsilon}}{(4\pi\Lambda^2)^{-\epsilon}} \frac{\Gamma(2-\beta-\epsilon)\Gamma(\alpha+\beta-2+\epsilon))}{\Gamma(2-\epsilon)\Gamma(\alpha)} \,. \tag{E16}$$

instead. More precisely

$$
\begin{aligned}
I_{(n_1+2-p_1)(n_2+2-p_2)(1-j_4)}&(a,b,e)\\
&= \int_p \int_q \frac{1}{(p^2+a)^{n_1+2-p_1}} \frac{1}{(q^2+b)^{n_2+2-p_2}} ((p-q)^2+e)^{j_4-1}\\
&= \sum_{q_1+q_2+q_3+q_4=j_4-1} \frac{(j_4-1)!}{q_1!q_2!q_3!q_4!} e^{q_4} \int_p \int_q \frac{(p^2)^{q_1}}{(p^2+a)^{n_1+2-p_1}} \frac{(q^2)^{q_2}}{(q^2+b)^{n_2+2-p_2}} (-2p\cdot q)^{q_3}\\
&= \sum_{q_1+q_2+2q_3+q_4=j_4-1} \frac{(j_4-1)!}{q_1!q_2!(2q_3)!q_4!} \frac{(2q_3)!}{q_3!} \frac{e^{q_4}}{(d/2)_{q_3}} \int_p \int_q \frac{(p^2)^{q_1+q_3}}{(p^2+a)^{n_1+2-p_1}} \frac{(q^2)^{q_2+q_3}}{(q^2+b)^{n_2+2-p_2}}\\
&= \sum_{q_1+q_2+2q_3+q_4=j_4-1} \frac{(j_4-1)!}{q_1!q_2!q_3!q_4!} \frac{e^{q_4}}{(d/2)_{q_3}} J_{n_1+2-p_1,-q_1-q_3}(a) J_{n_2+2-p_2,-q_2-q_3}(b)\,,
\end{aligned}
\tag{E17}
$$

where in the last steps we have used Eq. (E4).

For instance up to order μ^2, the gluon and ghost anomalous dimensions in the IR are found to be

$$
\begin{aligned}
\gamma_A =&\lambda \left\{ \frac{1}{3} - \frac{217}{180} \frac{\mu^2}{m^2} + \frac{4N_f}{5N} \frac{\mu^2}{M^2} \right\}\\
&+ \lambda^2 \frac{\mu^2}{m^2} \left\{ \frac{38687}{25920} - \frac{37}{288}\pi^2 + \frac{3647}{288} S_2 - \frac{179}{360} \ln \frac{\mu^2}{m^2} + \frac{13}{144} \ln^2 \frac{\mu^2}{m^2} \right.\\
&\quad + \frac{N_f}{N} \left[\left(\frac{8}{9} - 16x^2 + \frac{994}{9} x^4 - \frac{2756}{9} x^6 + \frac{520}{9} x^8 + \frac{7216}{9} x^{10} - \frac{1984}{3} x^{12} \right) \frac{\tilde{I}_{1xx}}{(1-4x^2)^4} \right.\\
&\qquad + \left(\frac{151}{90} - \frac{3334}{135} x^2 + \frac{3280}{27} x^4 - \frac{33112}{135} x^6 + \frac{3112}{9} x^8 - \frac{992}{3} x^{10} \right) \frac{\ln x^2}{(1-4x^2)^4}\\
&\qquad \left. - \frac{25 + 1122x^2 - 12128x^4 + 36760x^6 - 44640x^8}{270(1-4x^2)^3} \right]\\
&\quad + \frac{C_F}{N} \frac{N_f}{N} \left[-\left(\frac{16}{9} - 32x^2 + \frac{1952}{9} x^4 - \frac{5888}{9} x^6 + \frac{1664}{3} x^8 + \frac{1280}{9} x^{10} \right) \frac{\tilde{I}_{1xx}}{(1-4x^2)^4} \right.\\
&\qquad - \left(\frac{4 + 504x^2 - 8056x^4 + 47792x^6 - 78432x^8 + 19840x^{10} + 9600x^{12}}{135(1-x^2)^2} \right) \frac{\ln x^2}{(1-4x^2)^4}\\
&\qquad \left. \left. - \frac{4 - 416x^2 + 3904x^4 - 5376x^6 + 4800x^8}{135(1-4x^2)^3(1-x^2)} \right\}\,,
\end{aligned}
\tag{E18}
$$

and

$$
\begin{aligned}
\gamma_c =&\lambda \left(-\frac{5}{12} + \frac{1}{2} \ln \frac{\mu^2}{m^2} \right) \frac{\mu^2}{m^2}\\
&+ \lambda^2 \frac{\mu^2}{m^2} \left\{ -\frac{4295}{576} + \frac{5}{72}\pi^2 + \frac{459}{16} S_2 + \frac{1}{12} \ln \frac{\mu^2}{m^2} \right.\\
&\qquad \left. + \frac{N_f}{N} \left[\frac{5}{9} + 4x^2 + 4x^4 \tilde{I}_{1xx} + \left(\frac{1}{3} + 2x^2 \right) \ln x^2 \right] \right\}\,,
\end{aligned}
\tag{E19}
$$

where we have set $x \equiv M/m$. In deriving these expressions, we have used that $\psi_1(1/3) + \psi_1(1/6) = 8\pi^2/3 + 81 S_2$, where ψ_1 denotes the trigamma function. In the quenched limit $N_f \to 0$, we recover the results obtained in Ref. [37]. Similar (but lengthier) expressions can be obtained for the anomalous dimensions γ_ψ and γ_M.

[1] M. Peláez, M. Tissier and N. Wschebor, Phys. Rev. D **90**, 065031 (2014).

[2] D.J. Gross and F.J. Wilczek, Phys. Rev. Lett. **30**, (1973)

1343.

[3] H.D. Politzer, Phys. Rev. Lett. **30**, (1973) 1346.

[4] A. Cucchieri and T. Mendes, PoS LAT2007, (2007) 297.

[5] I.L. Bogolubsky, E.M. Ilgenfritz, M. Müller-Preussker and A. Sternbeck, PoS LAT2007, (2007) 290.

[6] A. Maas, Phys. Rev. **D75**, (2007) 116004.

[7] A. Sternbeck, L. von Smekal, D.B. Leinweber and A.G. Williams, PoS LAT2007, (2007) 304.

[8] I.L. Bogolubsky, E.M. Ilgenfritz, M. Müller-Preussker and A. Sternbeck, Phys. Lett. **B676**, (2009) 69.

[9] A. Cucchieri and T. Mendes, Phys. Rev. Lett. **100**, (2008) 241601.

[10] A. Cucchieri and T. Mendes, Phys. Rev. **D 78**, (2008) 094503.

[11] O. Oliveira and P.J. Silva, Phys. Rev. **D79**, (2009) 031501.

[12] Ph. Boucaud, J.P. Leroy, A.L. Yaounac, J. Micheli, O. Pène and J. Rodríguez-Quintero, JHEP **06**, (2008) 099.

[13] M. Q. Huber, Phys. Rev. D **101** (2020) no.11, 11.

[14] A. K. Cyrol, L. Fister, M. Mitter, J. M. Pawlowski and N. Strodthoff, Phys. Rev. D **94** (2016), 054005.

[15] M. Tissier and N. Wschebor, Phys. Rev. D **82**, 101701 (2010).

[16] V.N. Gribov, Nucl. Phys. **B139**, (1978) 1.

[17] G. Curci and R. Ferrari, Nuovo Cim. A **32**, 151-168 (1976).

[18] J. de Boer, K. Skenderis, P. van Nieuwenhuizen and A. Waldron, Phys. Lett. B **367**, 175-182 (1996).

[19] G. Curci and R. Ferrari, Nuovo Cim. A **35**, 1 (1976) [erratum: Nuovo Cim. A **47**, 555 (1978)].

[20] I. Ojima, Z. Phys. C **13**, 173 (1982).

[21] A. Cucchieri, T. Mendes and A. R. Taurines, Phys. Rev. D **71**, 051902 (2005).

[22] P. O. Bowman, U. M. Heller, D. B. Leinweber, M. B. Parappilly, A. Sternbeck, L. von Smekal, A. G. Williams and J. b. Zhang, Phys. Rev. D **76**, 094505 (2007).

[23] A. Cucchieri and T. Mendes, Phys. Rev. Lett. **100**, (2008) 241601.

[24] A. Cucchieri and T. Mendes, Phys. Rev. D **78**, 094503 (2008) doi:10.1103/PhysRevD.78.094503.

[25] M. Tissier and N. Wschebor, Phys. Rev. D **84**, 045018 (2011).

[26] M. Peláez, M. Tissier and N. Wschebor, Phys. Rev. D **92**, 045012 (2015).

[27] U. Reinosa, J. Serreau, M. Tissier and N. Wschebor, Phys. Lett. B **742**, 61-68 (2015).

[28] U. Reinosa, J. Serreau, M. Tissier and N. Wschebor, Phys. Rev. D **91**, 045035 (2015).

[29] U. Reinosa, J. Serreau, M. Tissier and N. Wschebor, Phys. Rev. D **93**, no.10, 105002 (2016).

[30] U. Reinosa, J. Serreau and M. Tissier, Phys. Rev. D **92**, 025021 (2015).

[31] J. Maelger, U. Reinosa and J. Serreau, Phys. Rev. D **97**, no. 7, 074027 (2018).

[32] J. Maelger, U. Reinosa and J. Serreau, Phys. Rev. D **98**, no. 9, 094020 (2018).

[33] U. Reinosa, Habilitation thesis [arXiv:2009.04933 [hep-th]].

[34] M. Tissier, Phys. Lett. **B784**, (2018) 146.

[35] J. Serreau and M. Tissier, Phys. Lett. **B 712**, (2012), 97.

[36] C. Noûs, U. Reinosa, J. Serreau, R. C. Terin and M. Tissier, SciPost Phys. **10**, 035 (2021).

[37] J.A. Gracey, M. Peláez, U. Reinosa and M. Tissier, Phys.

[38] J. I. Skullerud, P. O. Bowman, A. Kizilersu, D. B. Leinweber and A. G. Williams, JHEP **04**, 047 (2003).

[39] N. Barrios, M. Peláez, U. Reinosa and N. Wschebor, Phys. Rev. D **102**, 114016 (2020).

[40] J. C. Taylor, Nucl. Phys. B **33** 436 (1971).

[41] M. Peláez, U. Reinosa, J. Serreau, M. Tissier and N. Wschebor, [arXiv:2010.13689 [hep-ph]].

[42] M. Peláez, U. Reinosa, J. Serreau, M. Tissier and N. Wschebor, Phys. Rev. D **96**, no. 11, 114011 (2017).

[43] R. Alkofer and L. von Smekal, Phys. Rept. 353, 281 (2001).

[44] C. D. Roberts, M. S. Bhagwat, A. Holl and S. V. Wright, Eur. Phys. J. ST **140**, 53 (2007).

[45] M. Broilo, D.A. Fagundes, E.G.S. Luna and M.J. Menon, Eur. Phys. J. **C79**, (2019) 1033.

[46] D. Hadjimichef, E.G.S. Luna and M. Peláez, Phys. Lett. **B804**, (2020) 135350

[47] C.S. Fischer and R. Alkofer, Phys. Rev. **D67**, (2003) 094020.

[48] C.S. Fischer, and R. Alkofer, AIP Conf. Proc. **756**, (2005) 275.

[49] F. Gao, J. Papavassiliou and J. M. Pawlowski, [arXiv:2102.13053 [hep-ph]].

[50] P. O. Bowman, U. Heller, D. Leinweber, M. Parappilly, A. Williams, and others, Phys. Rev. D **70**, 034509 (2004).

[51] P. O. Bowman, U. Heller, D. Leinweber, M. Parappilly, A. Williams, and others, Phys. Rev. D **71**, 54507 (2005).

[52] A. Sternbeck, K. Maltman, M. Muller-Preussker and L. von Smekal, PoS **LATTICE2012**, 243 (2012).

[53] A. Ayala, A. Bashir, D. Binosi, M. Cristoforetti and J. Rodriguez-Quintero, Phys. Rev. D **86**, 74512 (2012).

[54] J. A. Gracey, Phys. Lett. B **552**, 101 (2003).

[55] R. M. Doria, Braz. J. Phys. 20, 316 (1990).

[56] D. Dudal, H. Verschelde and S. P. Sorella, Phys. Lett. B **555**, 126 (2003).

[57] N. Wschebor, Int. J. Mod. Phys. A **23**, 2961 (2008).

[58] S.P. Martin and D.G. Robertson, Comput. Phys. Commun. **174** (2006), 133.

[59] P. Nogueira, J. Comput. Phys. **105**, 279 (1993).

[60] S. Laporta, Int. J. Mod. Phys. **A15**, 5087 (2000).

[61] C. Studerus, Comput. Phys. Commun. **181**, 1293 (2010).

[62] A. von Manteuffel and C. Studerus, arXiv:1201.4330 [hep-ph].

[63] C.W. Bauer, A. Frink & R. Kreckel, cs/0004015.

[64] J.A.M. Vermaseren, math-ph/0010025.

[65] M. Tentyukov and J.A.M. Vermaseren, Comput. Phys. Commun. **181**, 1419 (2010).

[66] J.C. Collins and J.A.M. Vermaseren, arXiv:1606.01177 [cs.OH].

[67] See Supplemental Material for the electronic version of the 2-point functions written in terms of the master integrals.

[68] O.V. Tarasov and A.A. Vladimirov, Sov. J. Nucl. Phys. **25**, 585 (1977).

[69] É.Sh. Egorian and O.V. Tarasov, Theor. Math. Phys. **41**, 863-867 (1979).

[70] S. Weinberg, Phys. Rev. **118** 838-849 (1960).

[71] A. I. Davydychev, V. A. Smirnov and J. B. Tausk, Nucl. Phys. B **410**, 325-342 (1993).

[72] A. I. Davydychev and J. B. Tausk, Nucl. Phys. B **397**, 123 (1993).

[73] M. Caffo, H. Czyz, S. Laporta and E. Remiddi, Nuovo Cim. A **111**, 365 (1998).

[74] O. Oliveira, P. J. Silva, J. I. Skullerud and A. Sternbeck, Phys. Rev. D **99**, no. 9, 094506 (2019).

[75] T. van Ritbergen, J. A. M. Vermaseren and S. A. Larin, Phys. Lett. B **400**, 379-384 (1997).

[76] D. Binosi, J. Collins, C. Kaufhold and L. Theussl, Comput. Phys. Commun. **180**, 1709-1715 (2009).